University of South-Eastern Norway
Faculty of Technology, Natural Sciences and Maritime Sciences
Master´s Study
Master's in environmental science
2022

Kristian Louis Jensen

«Microplastic monitoring in freshwater and marine surface waters using Nile red and kayak paddling - a proposed study design for citizen science»

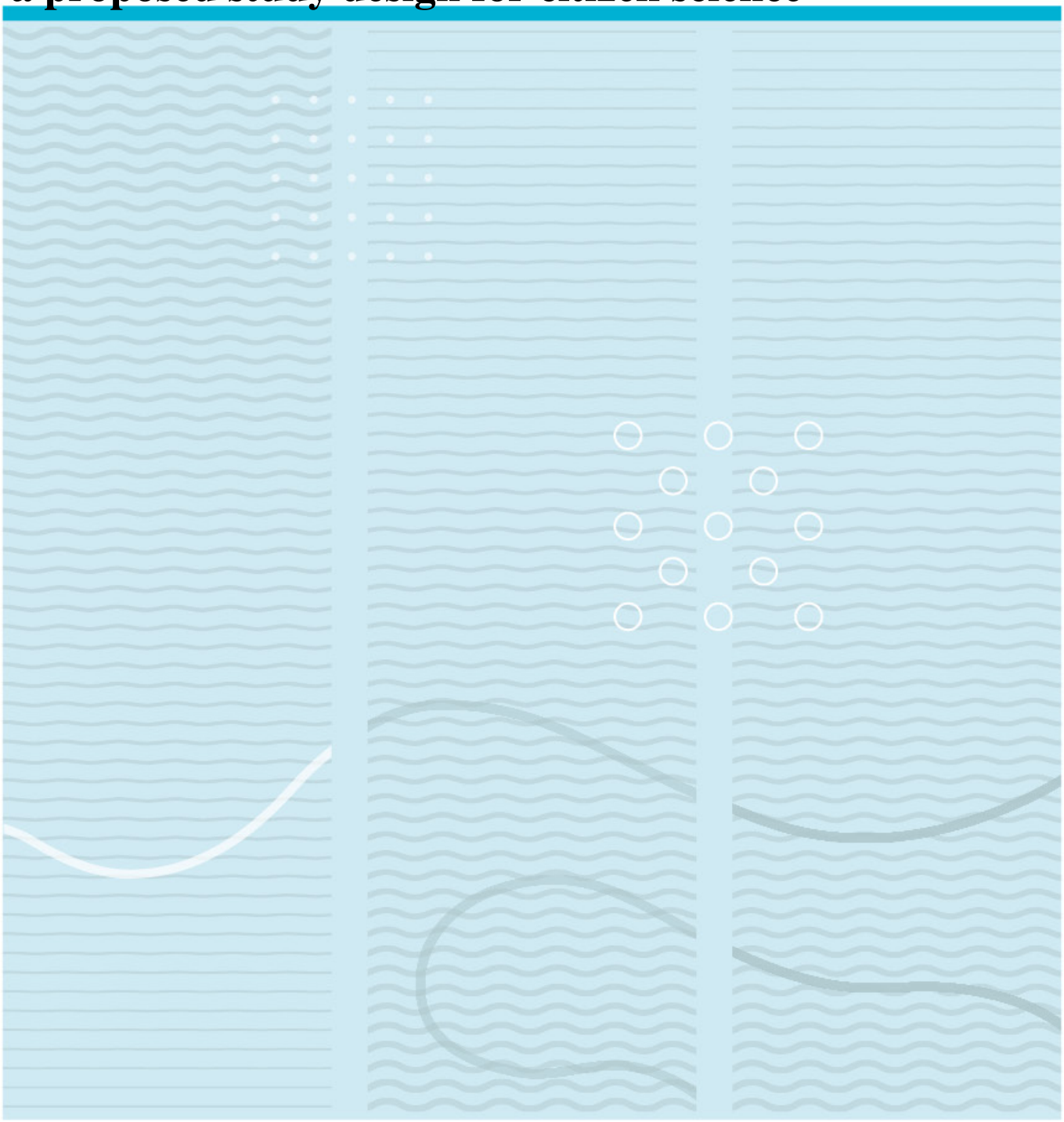

University of South-Eastern Norway
Faculty of Technology, Natural Sciences and Maritime Sciences
Institute of Natural Sciences and Environmental Health

PO Box 235
NO-3603 Kongsberg, Norway

http://www.usn.no

This thesis is worth 60 study points

Summary

The main aim of this master study has been to develop a cost-effective method to quantify microplastics in surface layers using a trawl towed from a kayak. The trawl was designed to sample microplastic in a wide range of aquatic ecosystems, including the marine Arctic. It seeks to raise awareness of freshwater, marine, and arctic microplastic pollution. The Plastsaq presented, is a modified neuston trawl capable of sampling microplastics in nearshore or difficult to access surface waters. This data collection by kayak, combined with subsequent Nile Red tagging of polymer particles and semi-automated scripts in ImageJ, allows for rapid microplastics screening. Microplastic data is presented from nearshore areas in the freshwater lakes of Southern Norway, marine waters of arctic Lofoten, Northern Norway, and Mediterranean samples from Barcelona and the Strait of Gibraltar. The data is used to describe potential differences in microplastic concentration as a result of different sources, e.g., nearby industry, inhabitants, or visitors to those areas. Our results provide insight into microplastic characteristics such as quantity, size, general distribution, and fragmentation dynamics. Obtaining data on these processes is a prerequisite for understanding how to mitigate the impacts of plastic pollution. This study allows to pinpoint sources of microplastics in nearshore environments by engaging the public in microplastic research.

Contents

Acknowledgements and preface

The formation of this Master´s study is a collaborative effort. Many parties were involved, including university supervisors, bachelor students, and an international network of scientists from Norway, the UK, and Spain. I have Greenlandic roots, which is the place where kayaking began, and through kayaking, I have first-hand seen the beauty of the marine world and why plastic debris is a real problem. Kayaking has allowed me to lead kayak tours professionally in some of the world´s most pristine places, such as Antarctica, Greenland, Costa Rica, and Norway. Unfortunately, in all these placed, plastic pollution was observed. Kayaking began with a purpose and allowed people to settle in the high arctic. The trawl we have developed could re-connect modern-day kayaking with a purpose.

Thomas Maes (GRID, Arendal), Synne Kleiven (USN), and myself developed this master study which aimed to develop a method for kayakers to sample microplastics in a cost-effective way using a Nile Red methodology. Synne Kleiven enrolled Rolf Thorkaas with his Bachelor project, “The Nile red method for identification of microplastic” (translated from Norwegian title).” His bachelor's study compliments this study. The collaboration between Rolf and myself has been incredibly beneficial for the development of this study. Rolf participated in some of the fieldwork and almost all lab work. This study would not have been possible without the support of the University of South-eastern Norway. I would like to thank Anna Vidal-Sanchez and the University of Barcelona, especially for the inspiration and hosting me in Spain and verifying the particles through FT-IR. Then, to Thomas Maes for outstanding mentoring, both in study design and the formation of the paper and for helping us to adapt and implement the Nile red technique in our university. To Laura Mendéz, who channeled my ideas through personal counseling, supported me with developing the R analysis, and gave advice and feedback on the document. To Frode Bergan for building, co-designing, testing, and teaching me how to build the “Plastsaq” prototypes 1, 2, 3 & 4. Finally, thanks to Synne Kleiven for outstanding mentorship and dedicated supervision of the whole study and steering it with such a focused, thoughtful, and helpful mindset.

Kristian Louis Jensen

Hopen, Lofoten 2022
Kristian Louis Jensen

1 Introduction

The generic term “plastic” encompasses many synthetic and semi-synthetic manufactured polymers used for almost all commodities and applications (Geyer, 2020). While invented in the 1950s, the overall production of plastics began in the 1970s. The high versatility, durability, and cost-effective production of plastics have made them a global industrial success story. Plastics are the result of polymerization or polycondensation of carbon and hydrogen molecules. Although made mainly from oil and gas some are also created from coal, natural gas, or natural carbon sources e.g., latex from trees and cellulose (Geyer, 2020). The worldwide production of plastics has dramatically increased since its invention, with global production reaching 367 million tons in 2020 and more than 300.000 different polymers produced (PlasticsEurope, 2021). Plastics intended life phase has qualities that have had a tremendously beneficial and positive impact on human population development because of plastics’ formability and bio-inertness. Therefore, it has significantly increased a wide array of public health parameters (Andrady et al., 2009). However, plastics’ un-intended life phase, caused by incomplete methods of discarding and recycling plastics, has resulted in a significant fraction of the produced plastics exists in the environment as mismanaged plastic waste (Jambeck et al., 2015a). Plastics have become a ubiquitously found persistent pollutant of emerging concern (Li et al., 2016; Persson et al., 2022). Studies suggest that there is a significant discrepancy between the amounts of mismanaged plastic waste and the current estimates in the marine environment. Based on observations estimates of floating plastic debris range between 14,4 – 269 metric tons (Cozar et al., 2014; Eriksen et al., 2014; Van Sebille et al., 2015). In 2015, the amount of plastic waste entering the ocean from land is estimated to be between 4.8 to 12.7 million metric tons (Jambeck et al., 2015a). The discrepancy is a debated issue, knowledge gaps include sources, sinks, pathways, and impacts of plastic pollution (Harris et al., 2021). Data coverage is too sparce, for example, coastal trapping of debris is rarely sampled, especially in the northern latitudes (Onink et al., 2021). Some polymers will stay afloat while other are too dense and will settle in sediments. Biofouling is also found to increase the density of the floating plastic, causing sedimentation (Kaiser et al., 2017). Different polymer types with additives will result in different temporal densities and cause sea column flotation or bottom sedimentation over time (Reisser et al., 2015). The knowledge we have of the abundance and behavior of floating plastic are primarily restricted to the open sea and the so-named plastic gyres (Law et al., 2010; Cozar et al., 2014). The primary sources of plastic to the environment are identified as mismanaged plastic waste, urban and stormwater runoffs, sewer overflows and wastewater treatment plants, in-or unintended littering, inadequate waste management from industrial activities, and car tires abrasions, construction, and illegal dumping from ships and fishery equipment. (Jambeck et al., 2015a).

Because of plastics' long life span, its adverse un-intended life phase will affect the world's aquatic ecospheres, likely for the next millennium (Van Sebille et al., 2012). Research into marine plastic pollution began in the Sargasso sea, far from the shore (Carpenter et al., 1972). The study found 3500 pieces of plastic, weighing 290 grams per square kilometer, with most pieces being between 0,25 and 0,5 centimeters in diameter. The size range below 5 mm would later be known as microplastic. The term was first coined by Thompson et al. (2004) in the first comprehensive study that sheds light on the adverse effect of plastic debris in this size range. To differentiate plastic in size groups, the following acknowledged categories are currently being used: macro- (>1 m) to meso- (> 5 mm), micro- (<5 mm), and nano- (<100 nm) plastic (GESAMP, 2016). Their tiny, almost imperceptible size range makes microplastics hard to study and observe, and science has struggled to enhance data mapping of abundance and concentrations. Microplastics can be classified into primary and secondary microplastics. Primary microplastics are intendedly small, produced plastic pellets, less than 5 mm, and are predominantly created for medicines, textiles, and personal care products (e.g., toothpaste, facial and body scrubs). Secondary microplastics are fragments of mismanaged plastic waste. It is considered that the majority of microplastics existing today are secondary microplastics (Cole et al., 2011), it follows that the increase of mismanaged plastic debris will increase the abundance of microplastics through fragmentation in the environment over time. Microplastics, both primary and secondary, are tremendously challenging to capture in wastewater treatment plants (Ziajahromi et al., 2017), and as a result escape water treatment process and enter the environments. There´s a consensus to limit plastics influx to the environment by suggesting mitigating actions, policies and measures targeting all levels of society, including the UN, EU and the general public (Napper et al., 2020). Nevertheless, future plastic production is expected to outweigh the effects of current mitigation strategies Borrelle et al. (2020). As research obtains more knowledge on the subject of microplastic, new discoveries are made, which can be exemplified by the study from Zimmermann et al. (2021), which found that consumers of everyday plastic items, e.g., household plastics, are exposed to higher and more chemicals from plastic than was previously thought. Due to higher leaching of chemicals from plastic studies in the laboratory than was expected. Plastics effect on human are still being poorly understood, but plastic debris has become a global issue of increasing concern with heavily documented harmful ecological and economic impacts (Geyer, 2020; Bergmann et al., 2022).

The plastic debris already present in the environment is in a state of continuing fragmentation into ever-smaller particles. Plastic debris fractionates due to environmental weathering, e.g., when exposed to UV radiation, mechanical abrasions & biotic interactions (Geyer, 2020). It has been shown

that plastic affects species differently in various size ranges and that size ranges have relative chances of bioaccumulation and different types of harm, for instance, when plastics size overlaps with the feeding size of an organism (Hidalgo-Ruz et al., 2012a; Jeyasanta et al., 2020). Microplastics are ubiquitous in all environments and have been found in surface waters, sediments, biota, in arctic glacial meltwater, in the Antarctic Sea, and on top of mountains (Browne et al., 2007; Kanhai et al., 2020; Kim et al., 2021). To tweak the properties of the polymers created, a wide variety of chemicals are added to improve their intended properties, known as additives (Hermabessiere et al., 2017). Adding to this, while microplastics are adrift in the ocean, they can absorb and transport persistent bio accumulative toxic compounds and organic pollutants (POPs) (Koelmans et al., 2013). Environmental microplastic is shown to exist as complexes with harmful environmental toxicants such as DDTs (Dichlorodiphenyltrichloroethane), organochlorine compounds, phthalates, dioxins, and other structured compounds (Yamashita et al., 2018). The ingestion of microplastic by biota can cause a range of effects, some are the result of the physical presence of the particle itself while others are resulting from the chemical composition of its additives or absorbed environmental pollutants. These effects include hampering of feeding, growth rates, reproduction, digestion, or enzymatic and hormonal production (Wright et al., 2013; Yin et al., 2021). In addition, microplastics are observed to increase the spread of invasive species using plastic as a vector and habitat, bacterial communities habituate floating plastics, and their plastics ocean transportation patterns could spread species globally (Aliani, 2003; Rech et al., 2016). The full range of detrimental effects we have yet to understand. However, the detrimental effects of plastic debris in natural ecosystems are significant and urge cautionary measures. (Botterell et al., 2020).

The current standard of analyzing and quantifying microplastics today are costly and complex. Many studies use labor-intensive methods such as visual inspection in combination with advanced chemical and physical characterization through electron microscopy. Visual inspection is counting different suspected plastic types based on color, shape, type of plastic, and degradation stage through the microscope. This method requires time consuming manual labor that, although educational, restrains widespread sampling. Visual sorting requires deep focus, might be prone to errors and is limited to larger particles (Mahtani et al., 2018). With electron microscopy and vibrational spectroscopy, plastic polymer determination is performed by chemical and physical characterization through absorption of light waves. Such as FTIR (Fourier Transform Infrared), which can be used to determine plastic down to its polymer type. It does so by comparing the spectrum of the sample with a database of spectral images. Based on this one can, with reasonable certainty, determine plastic polymer types. Raman micro spectroscopy is another common approach to determining microplastic polymer type. There

are studies that have begun to test the automatization of electron spectroscopy to decrease costs and precision for verification (Kappler et al., 2015; Tagg et al., 2015). But for large-scale microplastic research, this method will still be too costly, to adequately monitor sources and accumulation rates of microplastic. The analysis of microplastic remains costly due to the complexity of the machines and intensity of labor, to better address the plastic phenomena over the next century, fast and reliable ways to sample and analyze microplastic needs to be found, allowing to compare large datasets to understand the physical, chemical, and biological processes that influence plastic pathways. The analysis of microplastics with Nile Red dye is very promising for rapid screening of microplastics (Maes et al., 2017). Additionally, it can also be used as a precursor for more precise microplastic studies using spectroscopic techniques.

The laboratory part of this study uses a rapid-screening method with Nile Red, as developed by Maes (2017). Nile Red is a dye which renders certain plastic polymers fluorescent under a blue Crimelight emitter. Nile Red dye is an increasingly common dye used to quantify and identify microplastics (Maes, 2017; Lv et al., 2019; Prata et al., 2020; Meyers et al., 2022). It is a hydrophobic and metachromatic dye with the chemical formula 9-diethylamino-5H-benzo[alpha]phenoxazine-5-one. It was first used to visualize lipids by Greenspan et al. (1985). And because of NR´s ability to stain lipids, the dye alone, with no biological digestion or separation, leads to an overestimation of microplastics, ranging up to 100% (Stanton et al., 2019). But when pretreating samples, cleaning them from biological matter, either through chemical digestion or density separation, studies have shown that NR acts as a reliable way to make microplastic fluorescent under certain wavelengths. Nile red are shown to quantify more than 75% of the known environmental types of polymers, including Polystyrene (PS), Polyvinyl Chloride (PVC), Polyethylene terephthalate (PET), Polyethylene (PE) and Polypropylene (PP). Some studies are beginning to use the fluorescent colors to determine plastic polymers through semi-automated scripts (Meyers et al., 2022). Published studies that use a pretreatment e.g., organic matter digestion and/or density preparation in combination with Nile red have successfully identified microplastics.

To expand the environmental monitoring of microplastic and building spatial and temporal trends, there is an urgent need for a simple, cost-effective, and standardized way of sampling that provides data from a wide variety of aquatic ecosystems. To understand plastics abundance, distribution, and behavior we need large collaborative science projects that efficiently deliver data to execute mitigating strategies. We need harmonized protocols for sampling and sample treatments, that effectively quantifies microplastics (Geyer, 2020; Van Sebille et al., 2020). This proof-of-concept study uses the invented microplastics sampler, the “Plastsaq,” and Nile red fluorescent tagging. Once

stained, the microplastic samples are analyzed and data is produced by via script-based counts of particles in ImageJ (MP-VAT and MP-ACT). The idea to use a kayak was inspired by the citizen science approach of collecting microplastics data from Stand-Up paddle boards in the Mediterranean by Camins et al. (2020). Their long-term study based on a citizen science approach with stand-up paddlers successfully quantified microplastic in coastal areas in the Mediterranean Sea. In this study, we are advancing their research efforts by presenting a new trawl designed for kayaking, with a modified sample design strategy. The “Plastsaq” - is a modified neuston net pulled by a kayak to sieve surface-water layers for plastic using a 333 µm mesh net. The Plastsaq could increase microplastic sampling ranges in nearshore or difficult to reach areas while engaging the public in an educative manner.

Ending plastic pollution is no easy task, we are still observing an increase in plastic debris in marine and freshwater ecosystems (Jambeck et al., 2015a; Kasavan et al., 2021). Worldwide, legislators and governments are working together to mitigate the problem of plastic debris, demonstrated via the recent United Nations treaty entitled “End plastic pollution: towards an international legally binding instrument" (UNEP, 2022). Currently, we have limited microplastic data in nearshore, difficult to reach areas and higher latitudes, some of which are of interest to marine biodiversity. The approach presented in this study could cover these areas by using kayak communities that already co-exists with such areas. This simple and scalable data collection strategy together with the Nile Red staining protocol and automated counts through scripts, allows for rapid and cost-efficient screening of microplastics in a wide array of environments. We believe that this combination can increase societal understanding and public engagement into the problem of plastics as a permanent pollutant. If successful, this combination could significantly lower the costs of microplastic data gathering while involving the public in an empowering and educative manner.

2 Materials & Methods

First, an extensive literature search on plastics, microplastics and citizen science published up to November 2021was conducted to review relevant papers, books and articles using both library books and online databases such as Oria.no, Science Direct, Google Scholar and ResearchGate. The information was used to design and develop a methodology for microplastic sampling with kayaks, addressing the quality standards for microplastic monitoring. Keywords used in searches were: microplastics, marine microplastic analysis, microplastic research, citizen science, plastic fragmentation, plastic monitoring, marine debris, and plastics. This is the list of primary reference

papers for this master's study (Hidalgo-Ruz et al., 2012b; Nerland et al., 2014; Maes, 2017; Michida et al., 2019).

The study concept is based upon the study by Camins et al. (2020), using stand up paddle boards to monitor water surface microplastics in nearshore areas. Here, we aim to expand their efforts to develop a cost- effective microplastic monitoring approach by developing a trawl pulled by a kayak to sample microplastics. This study started in December 2020 when my father and I built a replica of the Camins et al. (2020) sample device (Figure 1). We trawled the device without a mesh net or cod-end to test its trawling safety from a kayak. We then conducted two marine trials to better understand how to gather samples in open sea. Following these trials, Frode Bergan, our university chief engineer, and I looked at the prototype and the drawings from Camins et al. (2020) and began researching literature on building the kayak prototype using available materials. Michida et al. (2019) and Prata et al. (2019) became our primary study and design inspiration sources. After conducting further freshwater and marine trials, the second prototype evolved from a manta

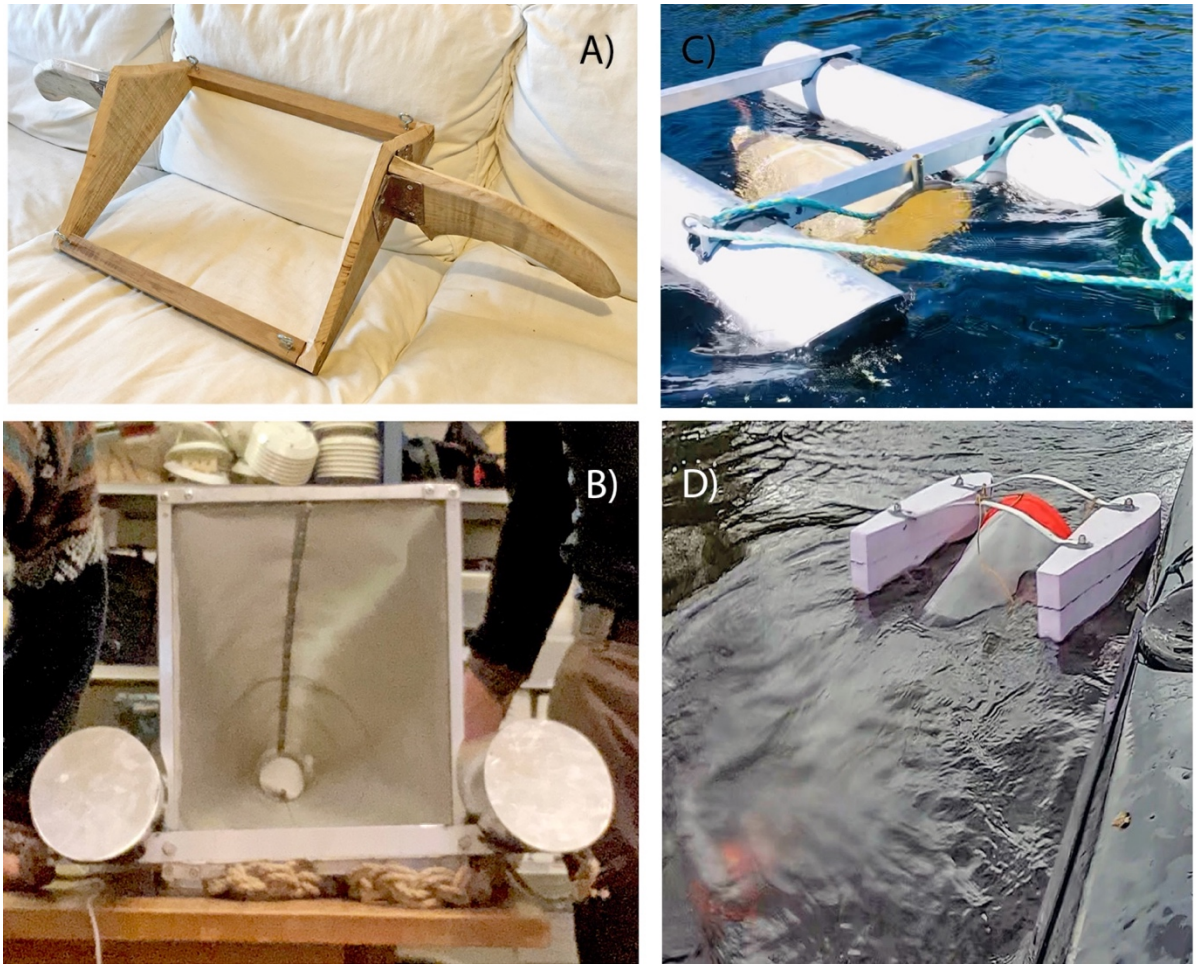

Figure 1 - Photographs of the different prototypes prior to designing the Plastsaq trawl.
A) The first prototype testing trawling safety from a kayak
B) The second prototype which still is in use for passive sampling of rivers
C) The third prototype in sampling test. D) Prototype with 30 cm net diameter in sampling test.
Photos: Kristian Louis Jensen

trawl type device into a neuston trawl layout. This second version reduced the drag needed and performed better in waves. A standard plankton trawl net with a diameter of 20cm proved to be the best size to achieve the sampling speed of 1.8-3.6 km/h (1-2 knots) reported by Michida et al. (2019). This final prototype allowed us to sample 1 km of water in approximately 20 mins.

2.1 The Plastsaq microplastic sampler

We named our final prototype, a modified neuston trawl for kayakers, the "Plastsaq" (Figure 2). This trawl was safe and practical to transport and deploy from a kayak. It is designed to sample large volumes of water for microplastics using kayaks. It could also be used from small vessels or boats. The Plastsaq resembles a neuston trawl (figure 3), the main floating body is made of Balsa wood, the lightest wood in the world, connected by two aluminum straighteners glued into the balsa wood.

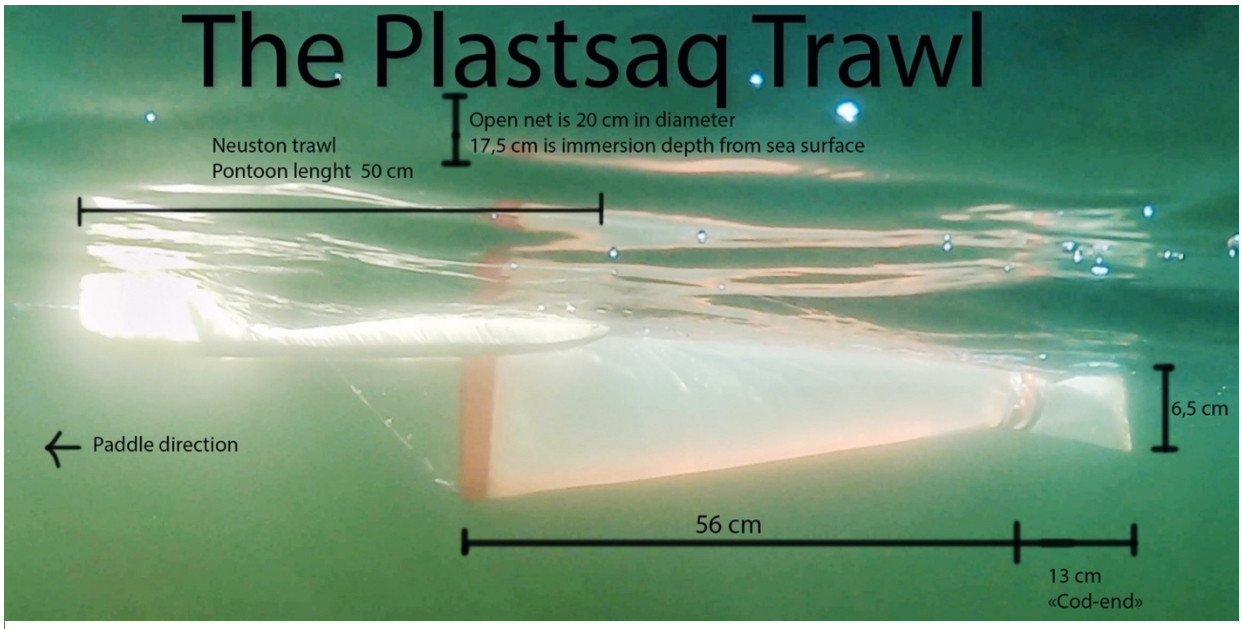

Figure 2 – In-sampling photo of the Plastsaq as proposed for microplastic sampling. The photo is marked with important measurements, proportions, and appearance of net in the water at 2,6 km/h speed. Photo: Rolf Thorkaas

The straighteners also hold the net, which has a net opening of 20 cm in diameter and funnels into a replaceable "cod-end." The mesh size of the net and cod-end is 333 μm. The extended net has a length of 56 cm with decreasing diameter. It attaches to a glass tube, 6,5 cm in diameter, with a length of 5 cm on which the "cod-end" is attached via an adjustable metal ring tightened by a flat screwdriver.

At a normal paddle pace, 2,6 km/h, the net is fully stretched and performing as desired. At this speed, the net allows particles to float into the cod-end naturally. We attached a flow-o-meter to the Plastsaq to measure the precise volume of water twice. This volume correlated closely to the water volume estimated using the net diameter and distance trawled. During sampling, the flowmeter was only used on two tours, and the volume was estimated via the calculations. We made a sampling comparison with the Plastsaq and the Camins et al. (2020) trawl at Barceloneta beach in Barcelona (figure 3). Both the Camins et al. (2020) device and the Plastsaq were trawled behind stand-up paddleboards at a much slower speed. The average speed with SUP was 1,8 km/h (1 knot) kayaks are twice as fast.

Figure 3 - Laura Galeano (Bachelor student UiB) holding the Camins et al., (2020) sample device and our trawl "the Plastsaq" at Barceloneta Beach (Spain). In this nearshore area close to Barceloneta beach in Barcelona we sampled the two-trawls side by side on a simultaneous sample. Photo: Kristian Louis Jensen

The Plastsaq can be easily transported onto a kayak because the width of the trawl and the back deck of a kayak (figure 4). The trawl is connected to the kayaker via a natural fiber rope connected to a

quick-release belt. The raft itself floats and the rope can be extended to desired length, 8 meters distance from kayaker to raft was used in this study.

Figure 4 - Different in-situ sampling photos of how the Plastsaq is used for sampling.
A) Rinsing the Plastsaq after sampling, using distilled water to flush all particles into the cod-end
B) Another angle of the Plastsaq showing the 20 cm opening C) How the Plastsaq is transported.
Photos: A) Rolf Thorkaas B) Evelyn Pecori C) Chris Eyre-Walker

2.1.1 Map of locations and sample strategy

Our main sampling strategy was to perform a 1000 meters trawl, at three locations at each site. (Figure 1). We would kayak with the Plastsaq on the back deck, to a suitable starting point, rinse the Plastsaq without a cod-end in the water for several minutes before attaching the cod-end. Then we would attach a clean filter to the net, and initiate Strava on phone and start paddling towards a point in the distance, in preferably a perpendicular direction to a suspected source of microplastics. When the Strava App confirms 1000 meters paddled, the Plastsaq is pulled in and cod-end marked and stored in pre-washed glass jars. Samples were obtained in Southern Norway, Arctic Norway, and the Mediterranean. Maps are presented as hybrid satellite images with local names and GPS data transect (Google Earth, modified trough Strava.com) All original gps data can be found online via (strava.com/athletes/80674195).

2.1.2 The sampling transects

All numerical data connected with the sampling are found in table 1.

Table 1 – overview of all sampling parameters connecting the sampling transects

Location	Date	Time	Start Coordinates	Distance on Strava	Weather	Wind Speed (m/s)	Wind Direction	Wind relation to transect	Current direction	Permanent Inhabitants n	Industry	Visitors pressure	Biological matter remova
Seljord 01	**28.08.2021**	**13:32 - 13:49**	**59°29'00.8"N 8°39'01.7"E**	**1000 meter**	**Fair**	**4**	**NE**	**No direction**	**Sideways**	**1430**	**No**	**Little**	**KOH:HCLO**
Seljord 02	**28.08.2021**	**14:13 - 14:32**	**59°28'35.5"N 8°38'38.8"E**	**1000 meter**	**Fair**	**4.3**	**ENE**	**No direction**	**Sideways**	**1430**	**No**	**Little**	**KOH:HCLO**
Seljord 03	**28.08.2021**	**14:53 - 15:12**	**59°28'50.8"N 8°40'30.5"E**	**1000 meter**	**Fair**	**4.4**	**ENE**	**No direction**	**Sideways**	**1430**	**No**	**Little**	**KOH:HCLO**
Notodden 01	**28.08.2021**	**19:46 - 20:04**	**59°33'30.7"N 9°14'39.6"E**	**1000 meter**	**Fair**	**6.6**	**NE**	**No direction**	**Sideways**	**9024**	**Yes**	**Little**	**KOH:HCLO**
Notodden 02	**28.08.2021**	**20:37 - 20:54**	**59°33'07.6"N 9°14'54.9"E**	**1000 meter**	**Fair**	**5.4**	**NE**	**No direction**	**Sideways**	**9024**	**Yes**	**Little**	**KOH:HCLO**
Notodden 03	**28.08.2021**	**21:08 - 21:24**	**59°33'15.4"N 9°13'47.4"E**	**1000 meter**	**Fair**	**5.2**	**NE**	**No direction**	**None**	**9024**	**Yes**	**Little**	**KOH:HCLO**
Gvarv 01	**14.11.2021**	**14:08 - 14:29**	**59°22'17.0"N 9°12'28.7"E**	**1000 meter**	**Fair**	**1.7**	**NNE**	**No direction**	**Sideways**	**1082**	**No**	**Little**	**KOH:HCLO**
Gvarv 02	**14.11.2021**	**14:47 - 15:08**	**59°21'31.7"N 9°11'49.9"E**	**1000 meter**	**Fair**	**1.7**	**NNE**	**No direction**	**Sideways**	**1082**	**No**	**Little**	**KOH:HCLO**
Gvarv 03	**14.11.2021**	**15:29 - 15:49**	**59°21'36.9"N 9°13'22.5"E**	**1000 meter**	**Breezy (5-8 m/s**	**6.5**	**ENE**	**Side wind**	**Sideways**	**1082**	**No**	**Little**	**KOH:HCLO**
Herøy 01	**29.08.2021**	**13:41 - 14:00**	**59°07'21.0"N 9°36'01.7"E**	**1000 meter**	**Fair**	**8.7**	**NE**	**No direction**	**Sideways**	**49265**	**Yes**	**Little**	**KOH:HCLO**
Herøy 02	**29.08.2021**	**14:33 - 14:49**	**59°06'28.6"N 9°37'04.8"E**	**1000 meter**	**Fair**	**8.4**	**ENE**	**No direction**	**Sideways**	**49265**	**Yes**	**Little**	**KOH:HCLO**
Herøy 03	**29.08.2021**	**15:06 - 15:23**	**59°06'22.9"N 9°35'09.8"E**	**1000 meter**	**Fair**	**7.8**	**ENE**	**No direction**	**None**	**49265**	**Yes**	**Little**	**KOH:HCLO**
Svolvær 01	**29.10.2021**	**13:12 - 13:28**	**68°14'06.6"N 14°34'44.4"E**	**1000 meter**	**Fair, sheltered**	**6.4**	**NW**	**Towards the wind**	**Against**	**4714**	**Yes**	**Medium**	**Density separation**
Svolvær 02	**29.10.2021**	**13:53 - 14:09**	**68°13'35.5"N 14°33'51.6"E**	**1000 meter**	**Fair, sheltered**	**6.4**	**NW**	**Towards the wind**	**Against**	**4714**	**Yes**	**Medium**	**Density separation**
Svolvær 03	**29.10.2021**	**14:16 - 14:34**	**68°13'07.2"N 14°33'37.9"E**	**1000 meter**	**Open Sea, swel**	**6**	**NW**	**Towards the wind**	**Against**	**4714**	**Yes**	**Medium**	**Density separation**
Kabelvåg 01	**24.11.2021**	**11:18 - 11:38**	**68°12'29.3"N 14°25'16.1"E**	**1000 meter**	**Sheltered bay,**	**6.8**	**NNE**	**Sidewind**	**None**	**2203**	**No**	**Medium**	**KOH:HCLO**
Kabelvåg 02	**24.11.2021**	**11:52 - 12:12**	**68°11'45.8"N 14°24'45.3"E**	**1000 meter**	**Sheltered sea,**	**7,2**	**NNE**	**Sidewind**	**Against**	**2203**	**No**	**Medium**	**KOH:HCLO**
Kabelvåg 03	**24.11.2021**	**12:25 - 12:45**	**68°11'29.8"N 14°23'22.7"E**	**1000 meter**	**Windstill sea in**	**6.9**	**NE**	**Sidewind**	**Against**	**2203**	**No**	**Medium**	**KOH:HCLO**
Reine 01	**27.11.2021**	**13:07 - 13:27**	**67°56'13.0"N 13°05'21.7"E**	**1000 meter**	**Fair, -9, frosty v**	**3.4**	**E**	**No direction**	**Sideways**	**311**	**Yes**	**Medium**	**KOH:HCLO**
Reine 02	**27.11.2021**	**14:10 - 14:30**	**67°56'42.2"N 13°07'53.7"E**	**1000 meter**	**Fair, -9, frosty v**	**3.2**	**E**	**No direction**	**With**	**311**	**Yes**	**Medium**	**KOH:HCLO**
Reine 03	**27.11.2021**	**14:42 - 15:02**	**67°57'06.0"N 13°05'38.7"E**	**1000 meter**	**Fair, -9, frosty v**	**3.3**	**E**	**No direction**	**Against**	**311**	**Yes**	**Medium**	**KOH:HCLO**
Gibraltar 01	**21.12.2021**	**14:27 - 14:46**	**36°08'31.8"N 5°21'53.6"W**	**1000 meter**	**Fair**	**3.7**	**E**	**Sidewind**	**Sideways**	**206701**	**Yes**	**High**	**KOH:HCLO**
Gibraltar 02	**21.12.2021**	**15:10 - 15:30**	**36°07'58.0"N 5°21'57.1"W**	**1000 meter**	**Fair**	**4**	**E**	**Sidewind**	**Sideways**	**206701**	**Yes**	**High**	**KOH:HCLO**
Gibraltar 03	**21.12.2021**	**15:56 - 16:13**	**36°06'27.4"N 5°20'51.7"W**	**1300 meter**	**Breezy**	**7.1**	**E**	**Sidewind**	**With**	**206701**	**Yes**	**High**	**KOH:HCLO**
Barceloneta (SFS)	**08.01.2022**	**12:24 - 14:14**	**41°22'27.9"N 2°11'28.5"E**	**1400 meter**	**Fair**	**8.2**	**NW**	**Sidewind**	**None**	**1,62 million**	**Yes**	**High**	**KOH:HCLO**
Badalona 01	**12.01.2022**	**12:17 - 12:36**	**41°25'31.0"N 2°14'15.6"E**	**1000 meter**	**Fair**	**7.6**	**ENE**	**Sidewind**	**Sideways**	**217741**	**Yes**	**High**	**KOH:HCLO**
Badalona 02	**12.01.2022**	**12:54 - 13:17**	**41°24'50.3"N 2°14'17.1"E**	**1000 meter**	**Fair**	**8.1**	**ENE**	**Sidewind**	**Sideways**	**217741**	**Yes**	**High**	**KOH:HCLO**
Badalona 03	**12.01.2022**	**13:55 - 14:14**	**41°25'54.7"N 2°14'32.8"E**	**1000 meter**	**Fair**	**2**	**ENE**	**No direction**	**None**	**217741**	**Yes**	**High**	**KOH:HCLO**

Below follows an observational account with satellite images of each sampling location following the logical order of the sampling. All satellite images are directed north, except Badalona which is directed north-west as depicted by north arrow in the top right of the image. Exact scale of satellite image is not available through strava.com output. All the sampling track figures have been made more visible and understandable by adding details to GPS track line. Blue arrows are added to the start of each sampling to mark the direction the sample was taken in. Two samples were longer than the rest. We sampled 1400 meters at Barceloneta beach when simultaneous sampling was followed by Camins et al. (2021). At the sample Gibraltar 03, the strong current of the Mediterranean made us paddle 1300 meters in 17 minutes. The samples are grouped in latitude dependent groups, first group, are from the inland of southern Norway (figure 5). Which were all performed in freshwater lakes near our university, here the first real samples were conducted. The samples follow a great water basin called “Skiens-vassdraget” and samples the lakes of Seljordsvannet, Heddalsvannet & Norsjø in the municipality of Telemark and Frierfjorden in Bamble municipality.

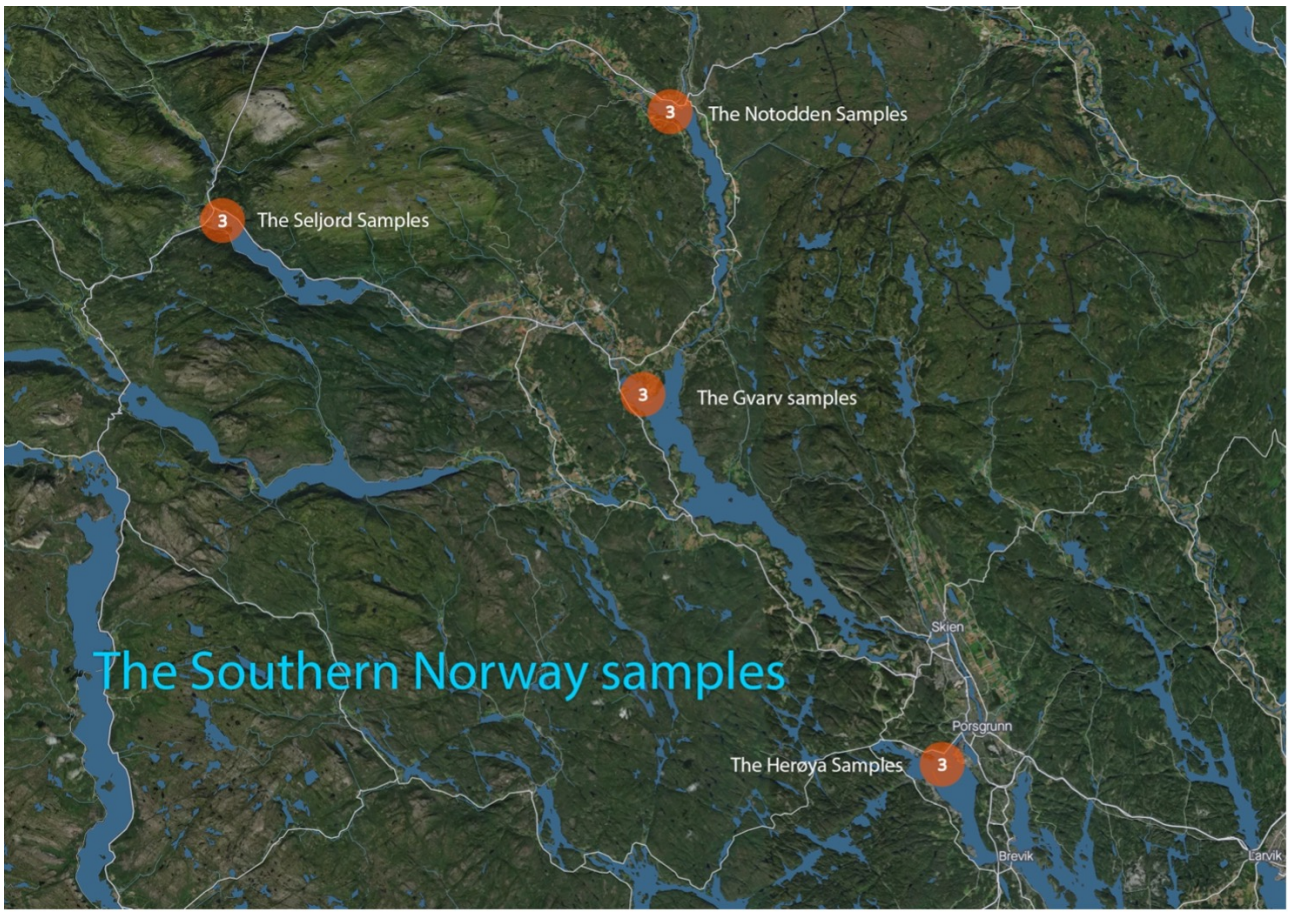

Figure 5 – Satellite overview of the areas of the southern Norway samples. Number depicted is number of samples within the orange circles.

The Seljord samples (figure 6) were performed in Seljordsvannet, a large freshwater lake close to the small settlement of Seljord, where 1430 permanent inhabitants reside (figure 3). The samples were performed in the northeast end of lake Seljordsvannet, close to the city of Seljord.

Figure 6 – Satellite image of the samples performed close to Seljord. The GPS sampling track is enhanced visually with orange lines. Paddling direction marked with blue arrow. Three 1000-meter samples were performed, in three different distances, perpendicular to incoming flow of the river.

The Notodden samples (figure 7) were performed at the northern end of Heddalsvatnet, in the region of Telemark. Here we sampled the river Tinnelva and its outflow into Heddalsvatnet. The river runs through Notodden, a larger settlement with 9024 permanent inhabitants. The river had a strong persistent inflow.

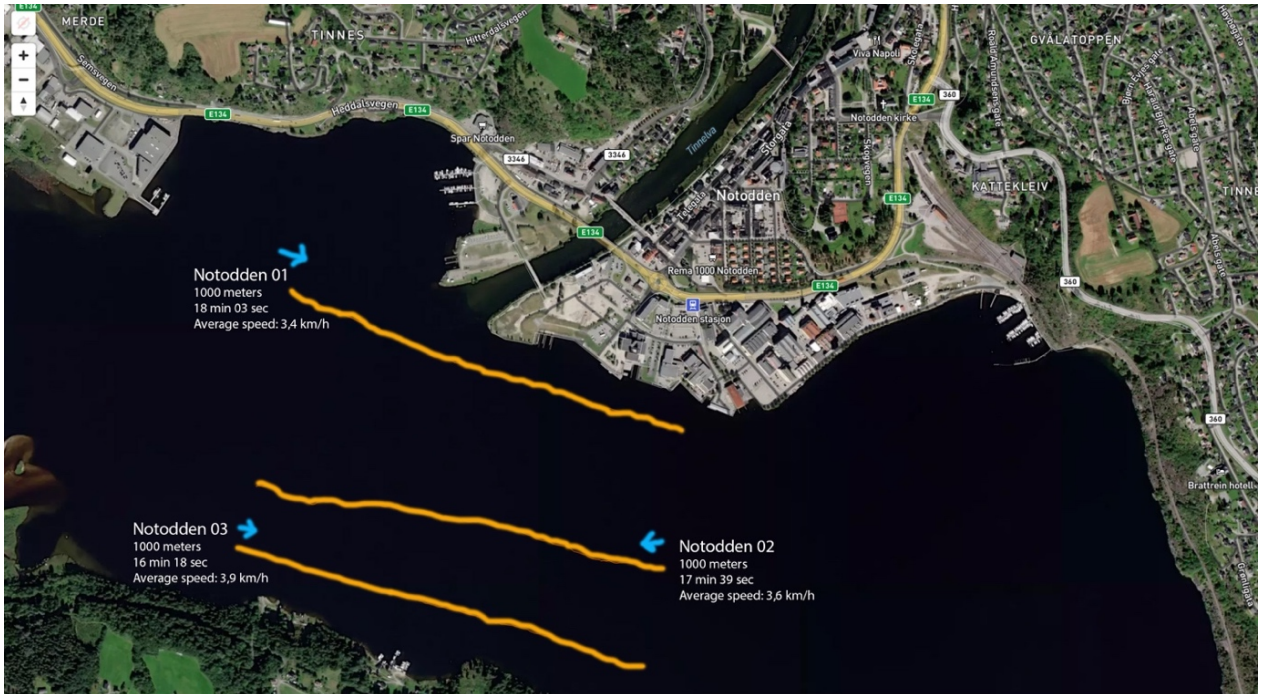

Figure 7 Satellite image of the samples performed close to Notodden. The GPS sampling track is enhanced visually with orange lines. Paddling direction marked with blue arrow. Three 1000-meter samples were performed, in three different distances, perpendicular to incoming flow of the river.

The Gvarv samples (figure 8) are performed in the lake of Norsjø in Telemark municipality, where the river Bø elva runs into the Norsjø lake. There is a nature reserve inside the bay, Årnesbukta. Upstream, the river meanders through a lot of terrain and several small settlements, including our university settlement of Bø and up towards Seljordsvannet where the first samples are taken. There is industry along the river.

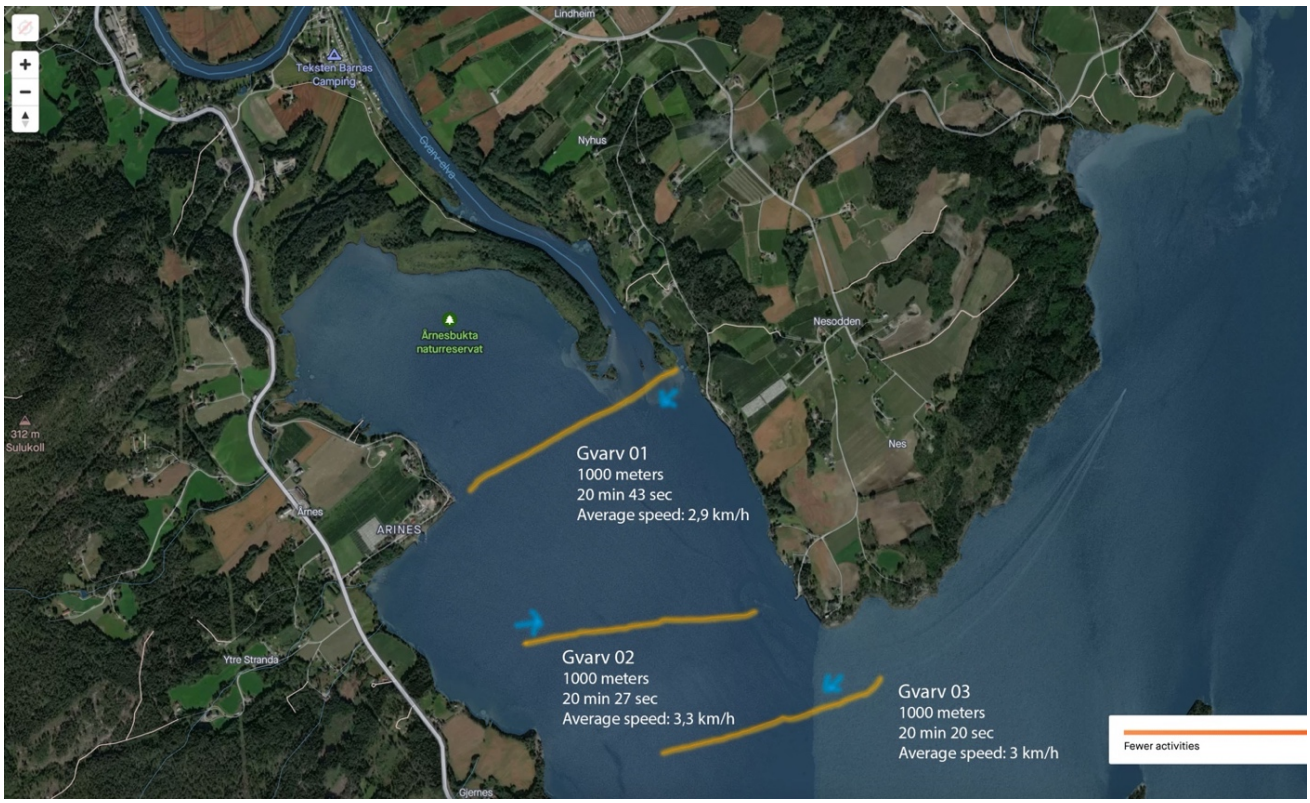

Figure 8- Satellite image of the samples performed close to Gvarv. The GPS sampling track is enhanced visually with yellow lines. Paddling direction marked with blue arrow. Three 1000-meter samples were performed, in three different distances, perpendicular to incoming flow of the river.

The Herøya samples (figure 9) are performed in "Frierfjorden" in the municipality of Bamble, where the river Skienselva, runs into Frierfjorden. Here we sampled in front of the large industrial zone of Herøya and performed three samples perpendicular to the river and the industrial park.

Figure 9 - Satellite image of the samples performed close to Herøya industrial park. The GPS sampling track is enhanced visually with orange lines. Paddling direction marked with blue arrow. Three 1000-meter samples were performed, in three different distances, perpendicular to incoming flow of the river.

The Lofoten samples (figure 10) were performed in Arctic Norway during the winter and spring months. These were our first marine samples. The samples were conducted in the municipalities of Vågan & Moskenes. Sampling in the Vestfjorden sea, a part of the Atlantic Ocean.

Figure 10 Satellite overview of location in Lofoten, Northern Norway in this study.

The Svolvær harbor samples (figure 11) were taken in the municipality of Vågan and were performed as one long kayak tour with three samples taken along the way. The first sample was in the harbor water that connects the town of Svolvær to the island of Svinøya. Sampling started under the bridge and then conducted three samples on the way out into the big sea of Vestfjorden. Aiming towards the island of Skrova in the sea of Høla, the northern part of the Vestfjorden sea.

Figure 11 Satellite image of the samples performed close to Svolvær. The GPS sampling track is enhanced visually with orange lines. Paddling direction marked with blue arrow.

The Kabelvåg samples (figure 12) were performed in Vågan municipality and were performed from the bay of "Ørsvågen" towards the beach of Silsand. This is a regularly conducted kayak tour and is performed by several kayak companies weekly. The samples serve as an experiment to see if the Plastsaq sampling could become part of a weekly kayak tour over one year.

Figure 12 - Satellite image of the samples performed close to Kabelvåg. The GPS sampling track is enhanced visually with orange lines. Paddling direction marked with blue arrow.

The Reine samples (figure 13) were conducted in the municipality of Moskenes in the Reinefjorden. Which is one of Norway´s most stunning fjords. The Reine fjorden samples were conducted as part of a winter kayak tour with ice in the harbor on a low light arctic day. It was– 11 degrees Celsius during paddling.

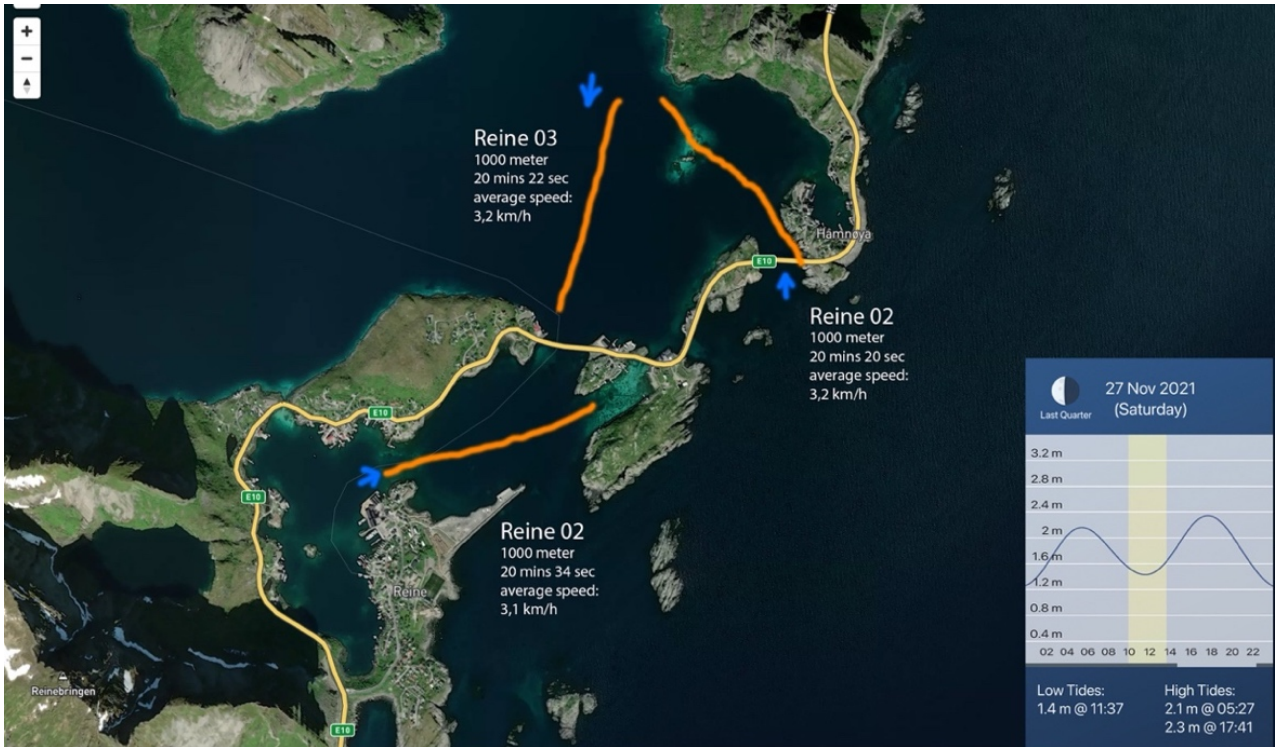

Figure 13 - Satellite image of the samples performed close to Reine. The GPS sampling track is enhanced visually with orange lines. Paddling direction marked with blue arrow.

The Mediterranean samples (figure 14) and their locations on the south-east side of the Iberian Peninsula.

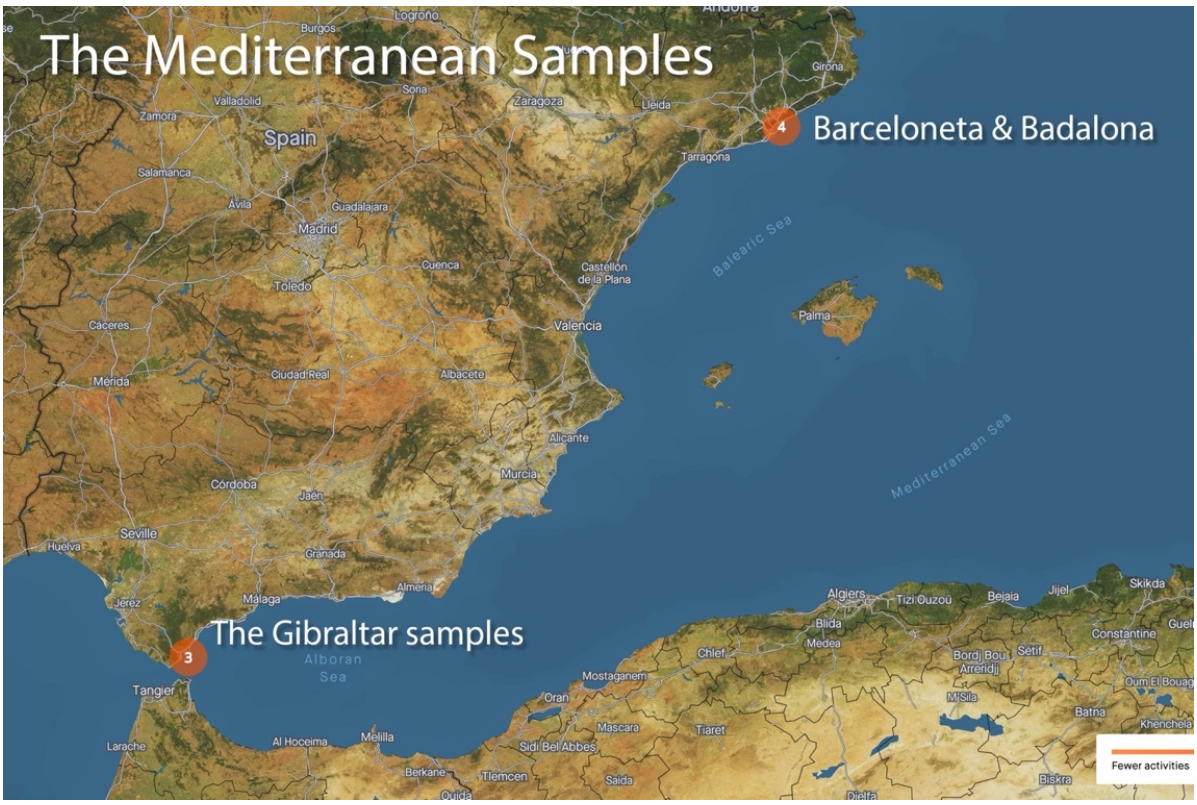

Figure 14 -Satellite overview of samples in the Mediterranean samples performed in this study.

The Gibraltar samples (figure 15) were all conducted as part of one kayak tour. In which we have collaborated with the local kayak club and sea conservation project “Nautilus” who believed that the wastewater dumped at the end of the island tip could perhaps be a microplastic source. The first sample was performed inside the harbor of Gibraltar, the next right outside it and the last where Nautilus suspected might be a source. The current of the strait took us be a surprise and suddenly we had paddled 1300 meters in only 17 mins.

Figure 15 Satellite image of the samples performed close to Gibraltar. The GPS sampling track is enhanced visually with orange lines. Paddling direction marked with blue arrow.

The Barceloneta samples (figure 16) were performed in the Ciutat Vella district of Barcelona in Catalonia, Spain, the beach of Barceloneta is perhaps Barcelona´s most popular and iconic beaches. In collaboration with Sanchez-Vidal et al. (2021) we compared the two trawl designs by doing a simultaneous paddling together with Laura Galeano of the University of Barcelona from two stand up paddle boards.

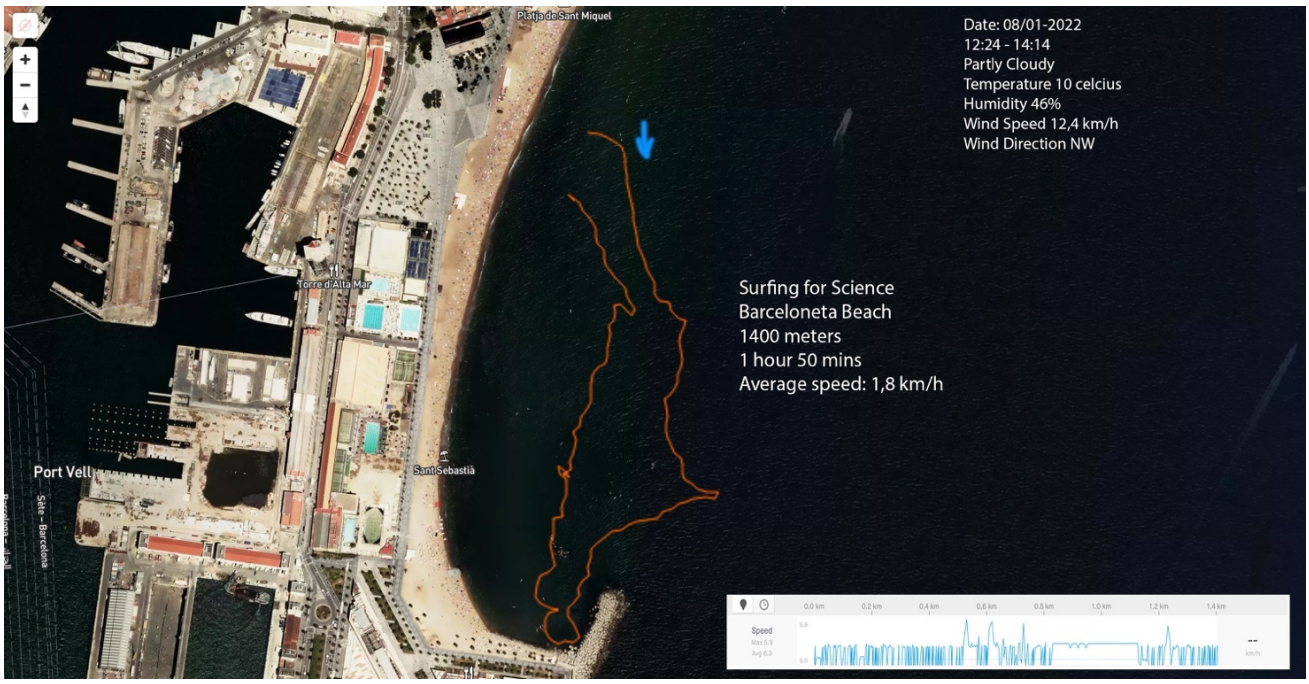

Figure 16 - Satellite image of the samples performed close to Barceloneta. The original GPS track is shown.. Paddling direction marked with blue arrow.

The Badalona samples (figure 17) were performed in the immediate northeast of Barcelona, in the city Badalona where the sampled the river Besós where it flows into the Mediterranean Sea. The river runs upstream through several large cities like La Garriga, Canovelles, Montmeló, Mollet del Vallès, Montcada i Reixac, Barcelona and Sant Adrià de Besòs.

Figure 17 - Satellite image of the samples performed close to Badalona. The GPS sampling track is enhanced visually with orange lines. Paddling direction marked with blue arrow.

2.2 Lab work

After each sample, we performed the following procedures to transfer the microplastic from the "Cod-End" sample filters. The sample filters were carefully extracted and cleansed of particles by spraying them with a distilled hand-water injector (ELGA purelab chorus, VEOLIA), transferring all materials from filters into glass beakers (1or 2-liter Borosilicate glass, 3,3, VWR). The best practice was to place the filter above the glass beaker, with the opening facing down, and spraying until all visual material and particles were washed out. Then the filters were turned inside out and rinsed until the filter re-gained pre-sampling appearance. This process was timed to take no less than 10 mins. And the results were carefully photographed. Varying amounts of distilled water were needed. E.g., we used 3 liters of distilled water in very dirty samples, e.g., Gibraltar 02, and some only required one liter (Ex Svolvær 01) to achieve pre-sample appearance. All original sample jars and lids were sprayed clean into the glass beaker to remove any particles that clung to the glass.

2.2.1.1 Removal/separation of biological matter

All except the three samples from the vicinity of Svolvær (figure 18) received the KOH: NaClO solution as proposed in Enders et al. (2017) study to remove organic matter. The 30% KOH: NaClO solution was prepared under a suction cabinet. The KOH pellets (Emsure, Merck) were saturated into a solution by mixing them with distilled water (1120 g KOH/L). They then mixed 1:1 with a solution with Sodium hypochlorite (14%, VWR) in an aqueous solution. The two solutions were mixed and 18,2 MΩ distilled water was added until a 30% KOH: NaClO 70% H_2O. *Note: The KOH pellets took 12 hours to dissolve in distilled H_2O under constant agitation. The chemical process creates an exothermic reaction, and the glass beaker was placed in a bath of ice to control heating up.*

All the sample containers were filled with 30%, depending on the volume of sample water, of the KOH: NaClO solution and placed in a 70 degrees Celsius heat cabinet under constant agitation using a magnetic stirrer for a minimum of 24 hours (Figure 10). After this process, all sample jars were stored inside a cold chamber for varying times until filtering began (sometimes a month). Because Nile Red is Ph sensitive (Maes, 2017), all the KOH: NaClO containing samples were buffered to a pre-decided neutral 7 (0.6) pH prior to filtering. Two methods to buffer the samples were used. The first method is to simply wash distilled water through the sample on the Whatman filter until the substrate water achieves the desired pH of 7 (0.6). The pH was measured with a standard pH meter (Radiometer analytical, PHM210) and calibrated with a pH buffer of pH four and pH seven. The second method was to drop sulfuric acid in drops while having constant agitation through a magnetic

stirrer and then constantly measure the pH in the sample water directly until the pH dropped from around 12,3 to 7 (0.6). This proved to be an easy way to get safe-to-handle samples.

2.2.1.2 Density separation

To apply the density separation method proposed by Maes (2017), the three "Svolvær" samples, which were low in organic material were used. Density separation was performed to separate biological matter from plastic particles using Zinc Chloride (Sigma-Aldrich, reagent grade 98%) to 1,37 mg/L density. The dense liquid was mixed with the sample substrate and poured into a conical glass separation Funnel (VWR, 1500 ml) as proposed in Maes (2017). With the conical glass, we could empty the sedimented bottom of the liquid after a minimum of 24 hours of sedimentation.

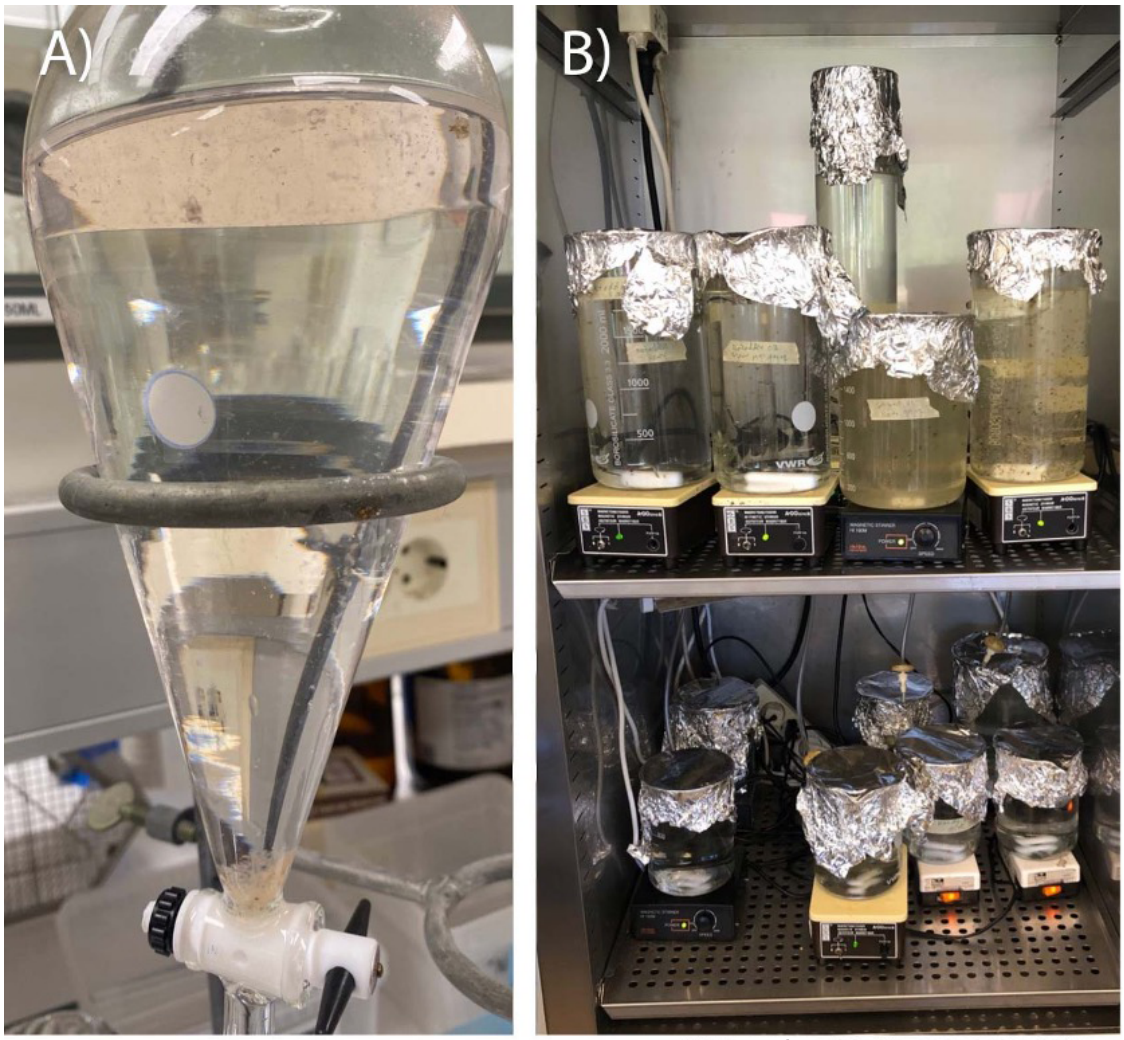

Figure 18 –A) Density separation according to the findings of Maes et al. (2017)
B) Biological matter removal with KOH: NaClO according to Enders et al. (2017)
Photos: Kristian Louis Jensen

2.2.2 Staining with Nile Red

After organic material digestion and the three-density separation treatments, all samples were vacuumed through a Whatman GF/D filter (2.7 um pore size, 90 mm, Cytiva, Whatman) and stained with Nile red (Sigma-Aldrich, technical grade, powder form). Nile red was mixed with acetone (EMSURE, ACS, ISO, REAG. pH) and then mixed with distilled water into a 10 ug/ml solution based on the findings of Maes (2017). The mixed Nile red solution was covered in aluminum foil and kept dark. 10ml Nile red solution was carefully added to the sample filter with a precise pipette (10ml, VWR) over the sample in the Whatman filter (still in the glass filtration funnel). The sample was then covered with aluminum foil and left to soak in the Nile red solution for 30 mins. Then it was vacuumed through, and the filter was carefully removed and placed onto a Petri dish. Then to dry the filters and make the fluorescent effect last longer, the filters were placed inside a heating cabinet (CARBOLITE) for 30 mins based on the findings Lv et al. (2019).

2.2.3 Photographing the filters

A black box was created (figure 19), using cardboard to create a suitable photographic environment and obtain an objective, replicable way to photograph the samples. The black box was placed inside a room that could be made almost dark during the daytime. The black box was big enough to encompass the university microscope (Zeiss Discovery.V20, Stereo) with Lens (Zeiss, PlanApo S, 1,0x, FWD 60mm) in a lab room used almost exclusively for this project, thus avoiding added contamination risks. A hole was cut on the black box so that the Crime-lite2 (420-470nm BLUE, Foster+Freeman) illuminated the sample filter at a 20 cm distance. We secured the orange fluorescence filter (529nm, Schott OG550 AG, 1% nom, cut off wavelength 550nm Foster+Freeman) on the microscope lens. the photos were acquired via the internal digital camera in the microscope (Zeiss, Axiocam 506 color).

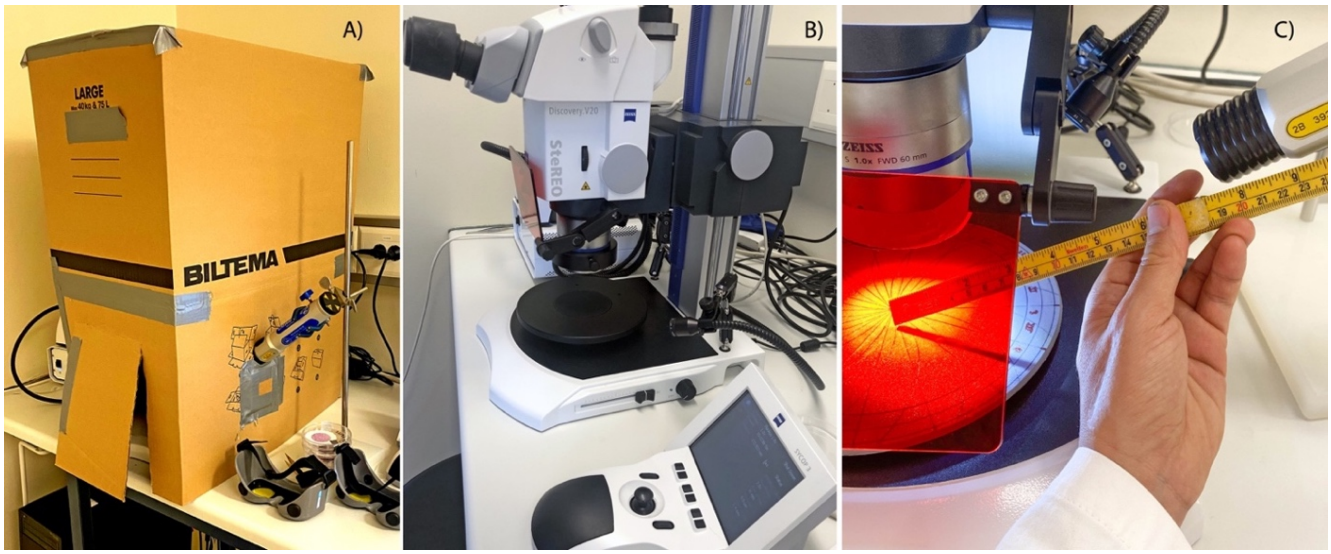

Figure 19 - A) The black box with the Crimelight attached.
B) The Discovery V.20, Carl Zeiss stereo microscope using to photograph the sample filters
C) The distance and placement of the Crimelight and the sample filters when photographing.
Photographs: Kristian Louis Jensen

Optimal photo settings are found in Prata et al. (2020) to be ISO 100, 2- second shutter time, aperture 5,6. We used these settings and took 8-12 images covering each part of the filter to later put them together into one high-resolution image of the whole filter. By stitching the photos together in the function "photomerge" in Photoshop, 2022.

Also, natural light photos of each sample filter were taken, allowing for direct comparison (figure 20). Samples were illuminated with the Zeiss CL 9000 LED at maximum emittance. The following settings were used for natural light: auto exposure (100% intensity, Binning 1*1, White auto balance). The images were exported as JPEG as a batch, in 100% quality. Each sample was named in series. (ex. Herøy01F1Nat). We then stitched the individual photos into a complete high-resolution image of all filters for analysis using Adobe Photoshop (2022) and ImageJ.

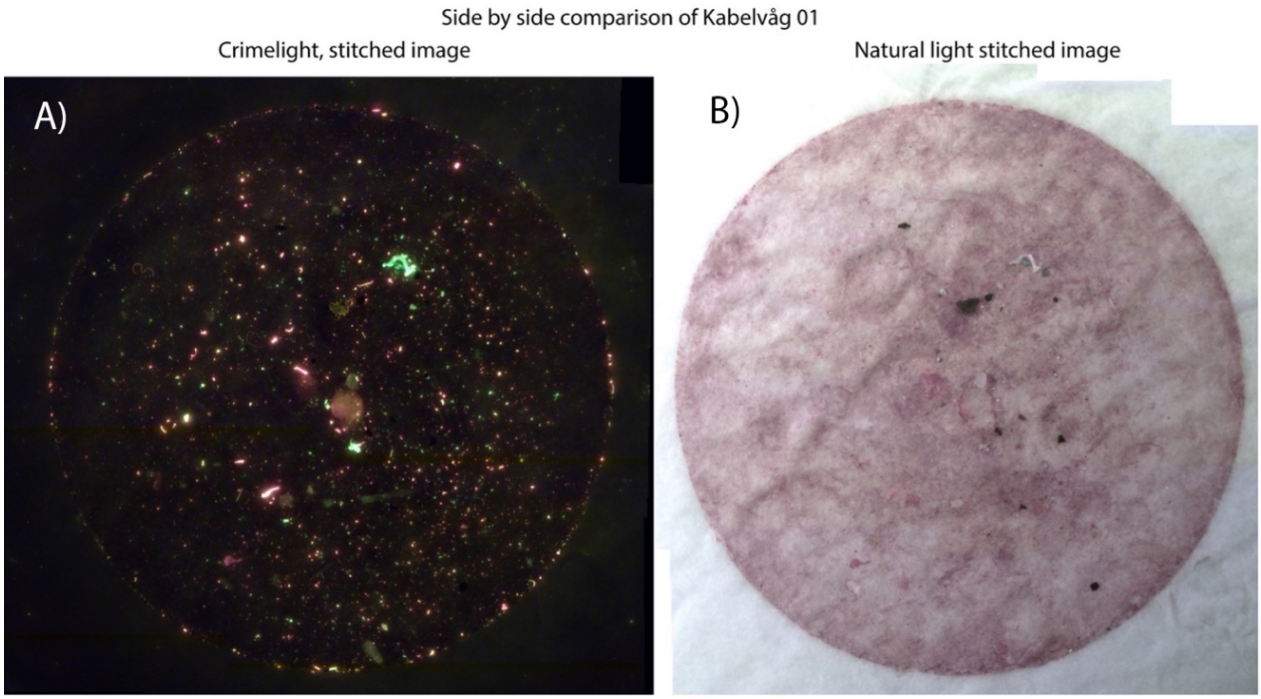

Figure 20 – Comparison of Kabelvåg 01 under crimelight and natural light.
A) How the filter appears when illuminated with Crimelight after Nile Red staining
B) How the filter appears illuminated with natural light after Nile Red staining
Photos: Kristian Louis Jensen

2.2.4 Handling data of the Nile Red stained images.

Once all photographs were downloaded and adequately named and were placed in adherent folders. Visual meta-analysis began of the engaging images. They were merged for complete visual comparison into a 15-gigabyte image called the “Giga photo” (figure 21). By having an overview of all the 44 filters, it was possible to evaluate and compare photographic conditions and visually compare the content of fluorescent microplastic in the samples. A structured library of sample filters, natural light filters, GPS data, and recorded speed was compiled, and exposure photographs were formed in conjunction with MP-ACT.

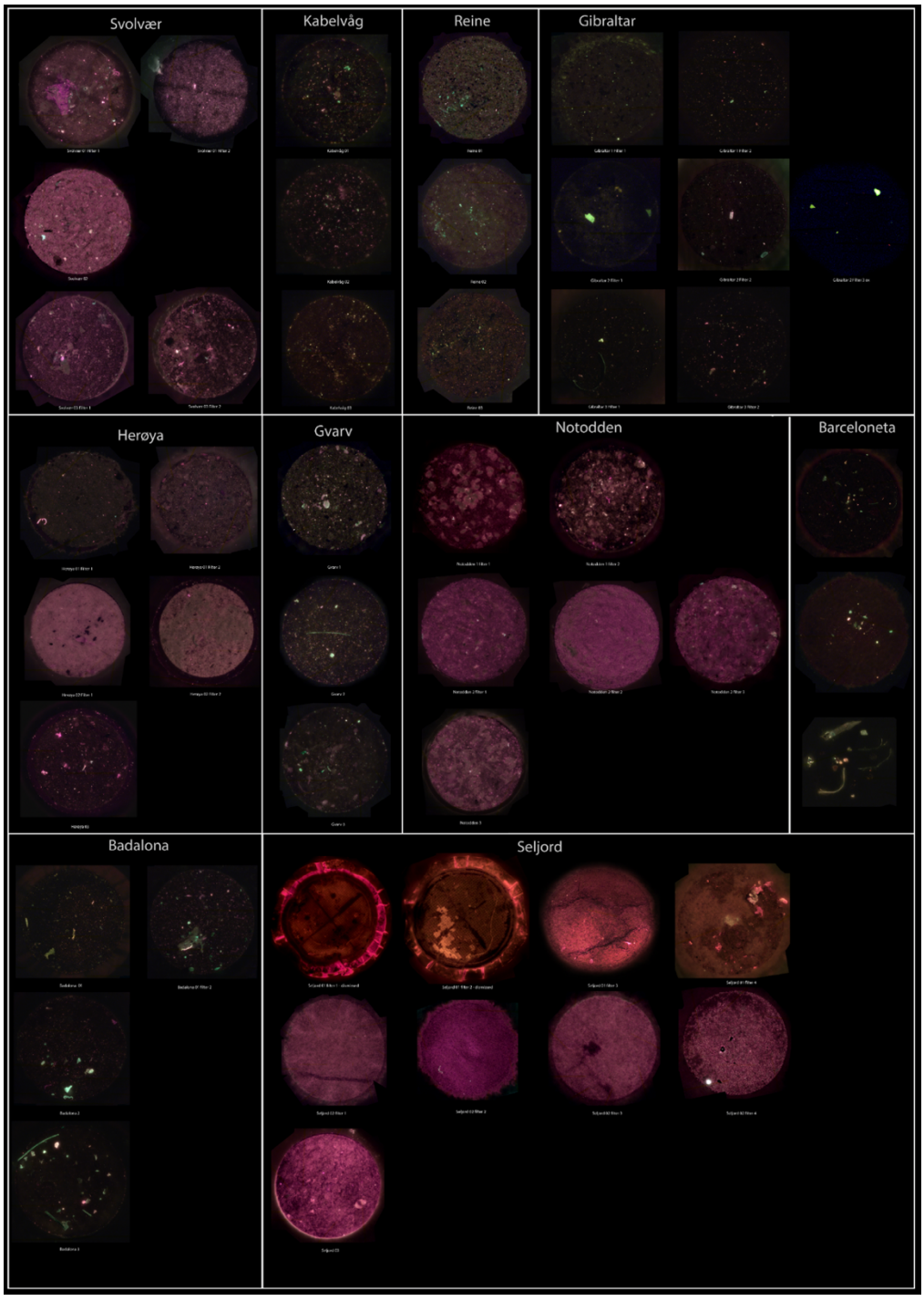

Figure 21 - The "Giga photo" - A full Resolution rendering of all our samples in their original resolution, making it possible to compare both photographic conditions but also the individual sample distance by zooming in and out of this giga photo. All sampled are vertically grouped. In first sample group, Svolvær, the two filters from Svolvær 01 are shown horizontally next to each other. Below is Svolvær 02 with one filter and so on. The two samples in Seljord 01, filters 01 and 02 were discarded due to wrong filter type that had fluorescent edges.

2.2.5 Microplastic quantification through ImageJ and MP-VAT & MP-ACT

The Nile Red stained images were analyzed by performing and comparing the two scripts developed by Prata et al. (2019). MP-VAT and MP-ACT. The two scripts quantify images by performing similar, simple, and precise pathways in ImageJ, with minor differences in the coded macro script. The pathways analysis is performed by selecting only the lightest areas of the images presented via a grayscale image conversion. The scripts then give light emittance a value between 0 (true black) and 100 (true white). It works by only selecting pixels over a certain light threshold, according to the observed range in the image. This allows precisely selecting only the fluorescent areas of images. Figure 22 shows the visual pathway of how particles are selected.

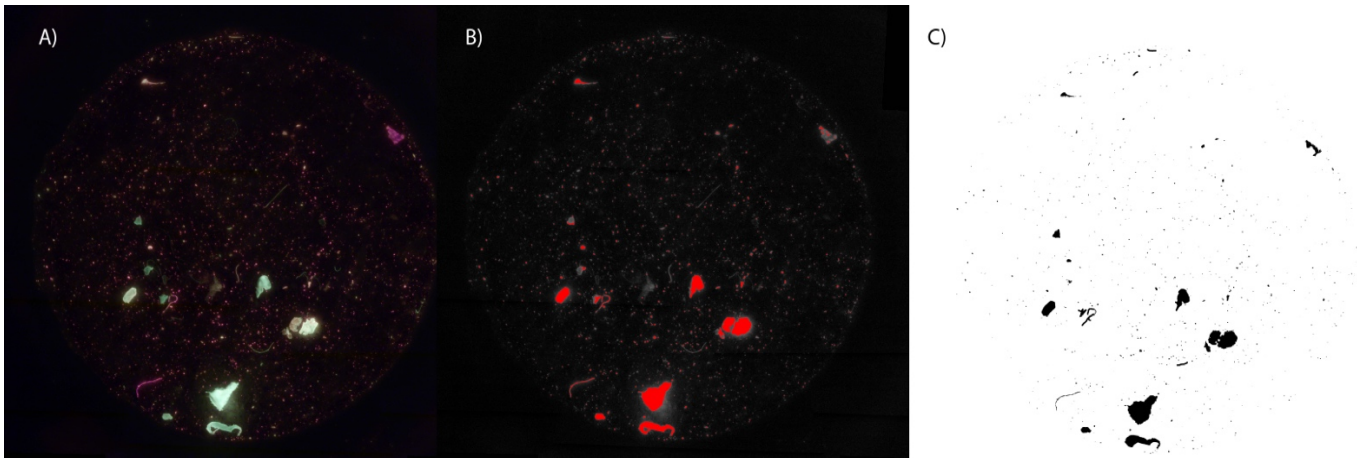

Figure 22 - A) Badalona02 Filter 1 Crimelight photo B) Same image fluorescence selection using MP-ACT C) Same selection of image as before but black and white.

MP-ACT performs by giving a manual selection on the threshold of the brightest parts of the image. It lets you visually select particle thresholds by user-controlled input. It also scales the image according to the known diameter of the filter, which MP-VAT does not. MP-VAT automates the process without user input and uses a pre-selected threshold of images called “MaxEntropy.” While investigating MP-ACT, it was discovered that one could digitally draw to enhance the selected areas of the images. Some of the bigger particles are fragmented on the edges, and the MP-ACT brush tool can precisely connect particles by drawing and connecting the fragmented parts. This added step can only be done to MP-ACT because MP-VAT automates this. MP-ACT allows for visual inspection of

the images according to photo exposure, and it is better at constraining the edges of particles by drawing them, as shown in figure 23. Connecting fragmented particles allows for higher precision of particle count. Some of our images were slightly overexposed, and it is then better to adjust the threshold according to exposure. This feature is lacking in MP-VAT. This emphasizes maintaining stable photographic conditions, as depicted in Prata et al. (2020). ImageJ produces data on the fluorescent tagging that converts the selection data into an Excel file. The data it gives is the area in scaled mm, feret sizes, roundness, an estimate of particle/fragment/fiber, and number.

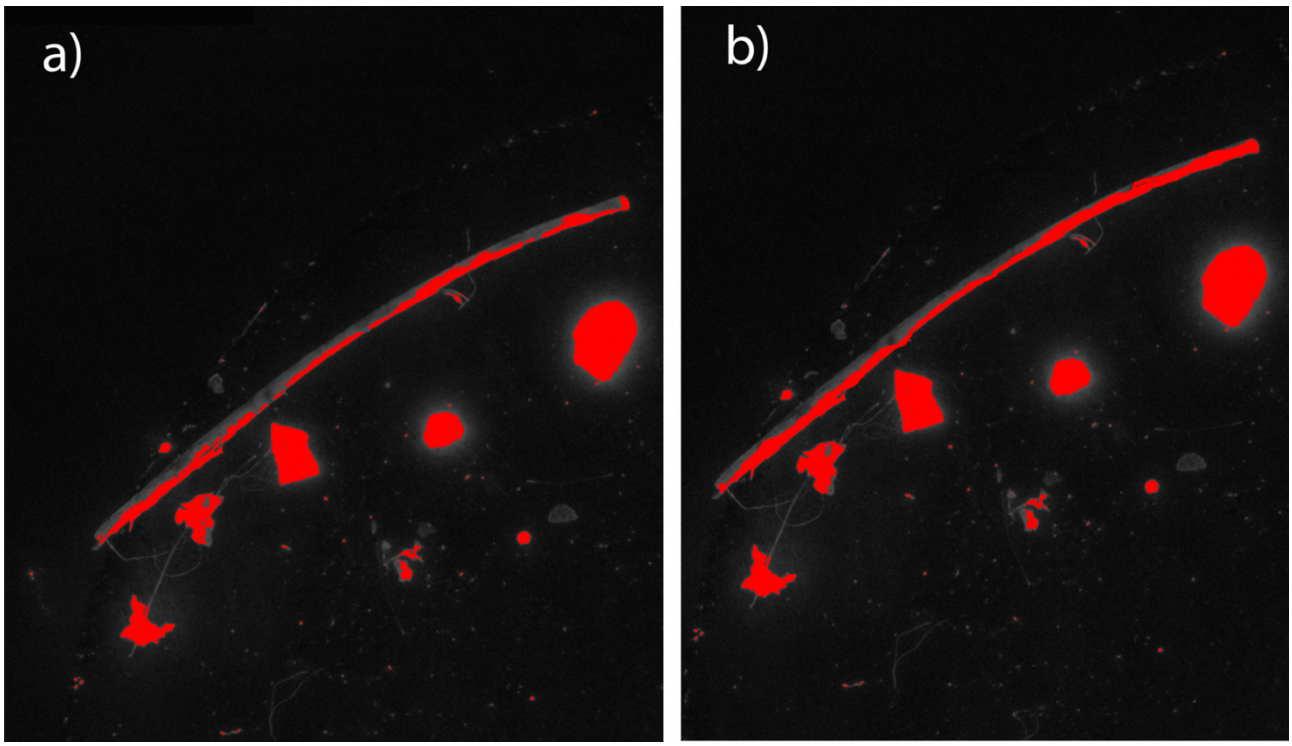

Figure 23 – Crimelight images of a part of Badalona 03 Nile red stained filter.
a) Showing the selected particle using the ImageJ script MP-ACT, the long piece of plastic here is fragmented such that it counts several particles instead of one. b) how the problem can be solved inside ImageJ by connecting the fragmented particles by drawing the area together.

The data was then run through statistical analysis and presented as a histogram of particle counts with all transects visualized with the two different model estimations of MP. To show the differences between sampled areas regarding the number of microplastics, we performed boxplots to visualize the max, min, and median of different groups of values. We also grouped them as three replicas of each location and then grouped the locations into latitude-dependent bulks: the Arctic, Southern Norway, and the Mediterranean.

2.2.6 FT-IR verification

To verify that the fluorescent particles identified by the Nile Red technique were indeed microplastics, 42 particles were extracted (figure 24) the particles were randomly selected via a

random number generator of large enough particles across all sample filters. Organized via a plastic particle organizer with different compartments for the individual particles with markings. The plastic particle organizer was brought with me from Bø to Barcelona. In Barcelona, we used FTIR machines or Fourier transform Infrared spectroscopes. FTIR machines work by shining a beam of light with numerous frequencies and measuring how much of the beam of light is absorbed by a sample. It then beams a different set of light frequencies at the sample and measures the absorption and the difference between the two beams. This produces a spectrum image showing which wavelengths the sample absorbs the beam of light. The spectrum image allows the observer to identify which compound it is. FTIR was used to determine whether the Plastsaq sample particle was organic in origin or was a plastic polymer. FTIR may only determine particles of a specific size, <5 mm. The 42 particles were analyzed on an FT-IR Spectrometer (Frontier, PerkinElmer) at the University of Barcelona under the supervision of Anna Vidal-Sanchez and machine operators.

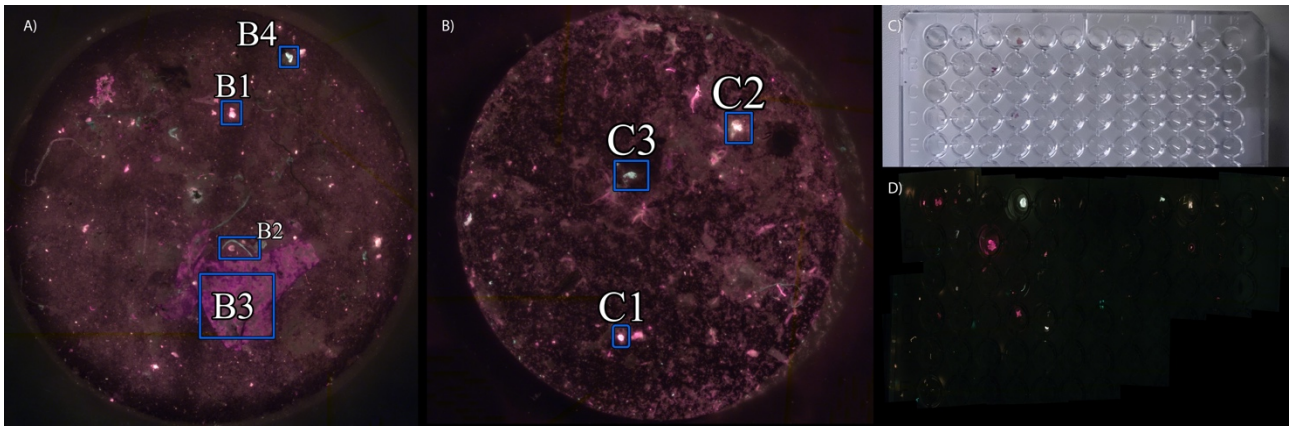

Figure 24 - Illustrating how we selected and transported 42 particles to Barcelona
A) The particles selected from Svolvær 01 Filter 1 chosen and their place in the organizer of particles. B) Particles selected from Svolvær 03 Filter 2.
C) The organizer of particles in natural light D) The organizer of particles under crimelight.
Photos: Rolf Thorkaas & Kristian Louis Jensen

2.3 Contamination measures

Because microplastic research is not yet permanently established at our university, no actual clean room for microplastic research was established. But we have done our utmost to limit sources of microplastic contamination by washing all sampling equipment with distilled water and acetone before usage and testing for particles and contamination sources in our sampling equipment, such as the kayaks and air of the laboratory. This was done to better understand the sources of microplastic contamination at our facilities inside the University for future studies. A series of contamination tests were performed. Most are done and presented in the adhering study from Thorkaas (2022). We have

tested the available sampling equipment, such as the kayak, rope, cardboard, and lab coat, as shown in figure 25.

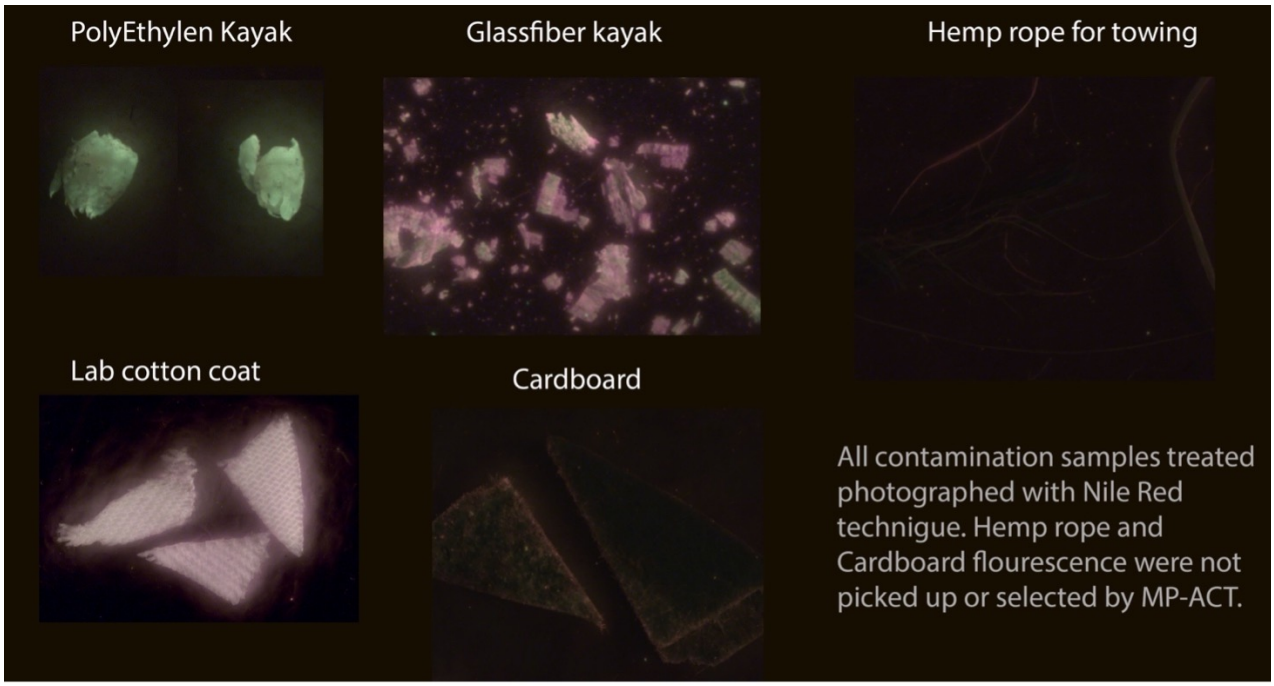

Figure 25 - The Nile Red stained contamination tests from sampling and laboratory equipment.

A filter was exposed to open air when samples were treated (figure 26), called the airborne microplastic filter. The full range of Nile Red adaptations and contamination considerations are found in the supporting bachelor thesis in Rolf Thorkaas (2020). We have done our utmost to investigate

and to learn from using Nile Red and the potential contamination of microplastics. Our contamination tests are furthered in the adherent paper from Thorkaas (2022).

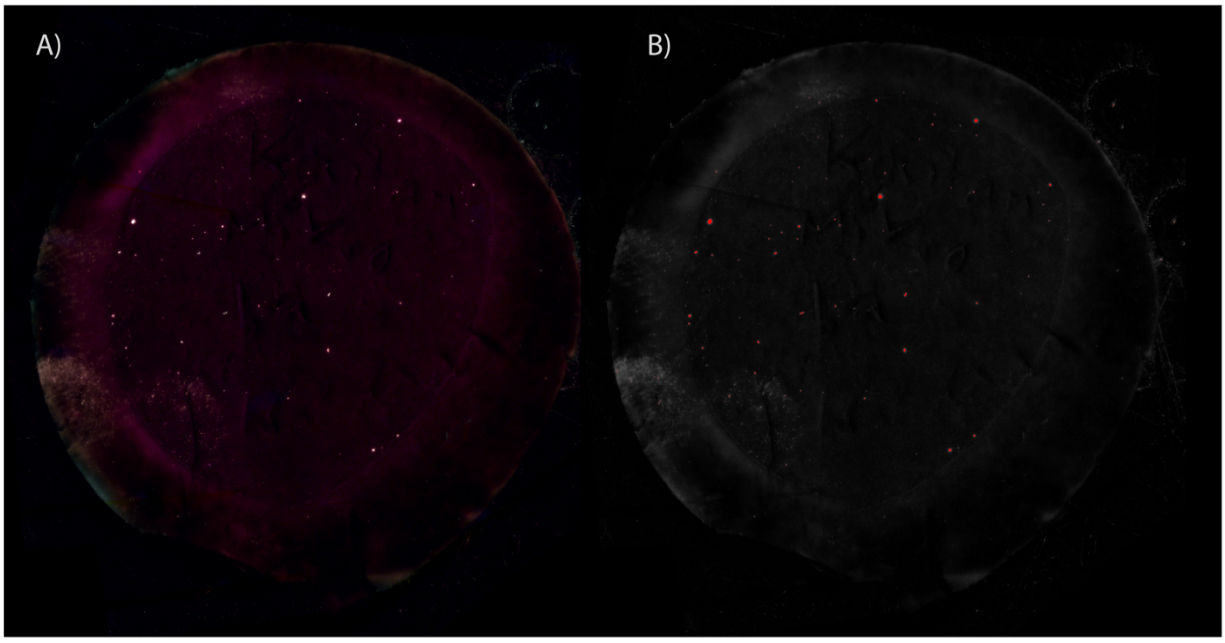

Figure 26 – Open-air contamination filter - which was open when samples were exposed to air in the lab and both samples and the filter were enclosed in aluminum foil between processes. A) The open-air contamination filter Nile red stained under crimelight. B) The particles selected by the scripts.
Photos: Kristian Louis Jensen

2.4 Statistical analysis

2.4.1 Predictor variables

To choose possible predictor variables, notice was kept of the apparent variables in situ, such as wind speed and current direction according to sample direction, duration of sampling. Numerical variables were added such as inhabitants, industry in the proximity and how we removed organic matter from the samples. When performing R analysis, the complete list of predictor variable was reduced to a selection of candidate predictor variables, as shown in figure 2.

Table 2 - Overview of sampling parameters used as predictor variables in this study

Sampling	Location	Inhabitants	Industry	Visitors	Particle_MPACT	Particle_MPVAT	Particles_pr_m3MPACT	Particles_pr_m3MPVAT	Duration_min	Total_MP_Area_mm	Latitude
1Seljord	Seljord_01	1430	No	Little	384	216	12.22	6.88	17	7.46	South.Norway
1Seljord	Seljord_02	1430	No	Little	364	1245	11.59	39.63	19	9.99	South.Norway
1Seljord	Seljord_03	1430	No	Little	199	182	6.33	5.79	19	2.22	South.Norway
2Notodden	Notodden_01	9024	Yes	Little	381	464	12.13	14.77	18	16.11	South.Norway
2Notodden	Notodden_02	9024	Yes	Little	650	384	20.69	12.22	17	25.71	South.Norway
2Notodden	Notodden_03	9024	Yes	Little	103	120	3.28	3.82	16	4.26	South.Norway
3Gvarv	Gvarv_01	1082	No	Little	2482	2823	79	89.86	21	57.54	South.Norway
3Gvarv	Gvarv_02	1082	No	Little	877	963	27.92	30.65	21	16.53	South.Norway
3Gvarv	Gvarv_03	1082	No	Little	1027	159	32.69	5.06	20	24.71	South.Norway
4Heroy	Heroy_01	49265	Yes	Little	1243	1293	39.57	41.16	19	16.99	South.Norway
4Heroy	Heroy_02	49265	Yes	Little	253	259	8.05	8.24	16	3.3	South.Norway
4Heroy	Heroy_03	49265	Yes	Little	807	880	25.69	28.01	17	19.28	South.Norway
5Svolvar	Svolvar_01	4714	Yes	Medium	754	549	24	17.48	16	22.92	Arctic.Norway
5Svolvar	Svolvar_02	4714	Yes	Medium	467	522	14.87	16.62	16	14.92	Arctic.Norway
5Svolvar	Svolvar_03	4714	Yes	Medium	521	592	16.58	18.84	8	20.39	Arctic.Norway
6Kabelvag	Kabelvag_01	2203	No	Medium	561	602	17.86	19.16	20	9.92	Arctic.Norway
6Kabelvag	Kabelvag_02	2203	No	Medium	777	849	24.73	27.02	20	16.86	Arctic.Norway
6Kabelvag	Kabelvag_03	2203	No	Medium	778	807	24.76	25.69	20	8.16	Arctic.Norway
7Reine	Reine_01	311	Yes	Medium	789	346	25.11	11.01	20	8.52	Arctic.Norway
7Reine	Reine_02	311	Yes	Medium	691	756	22	24.06	20	8.12	Arctic.Norway
7Reine	Reine_03	311	Yes	Medium	1038	1095	33.04	34.85	20	9.7	Arctic.Norway
8Gibraltar	Gibraltar_01	206701	Yes	High	810	209	25.78	6.65	19	10.63	Mediterranean
8Gibraltar	Gibraltar_02	206701	Yes	High	2406	1127	76.59	35.87	20	38.75	Mediterranean
8Gibraltar	Gibraltar_03	206701	Yes	High	1077	355	26.37	8.69	17	25.46	Mediterranean
9Barcelone	Barceloneta	1620000	Yes	High	1059	236	24.08	5.37	110	168.44	Mediterranean
9CBadalon	Badalona_01	217741	Yes	High	1680	449	53.48	14.29	19	57.22	Mediterranean
9CBadalon	Badalona_02	217741	Yes	High	852	943	27.12	30.02	23	26.09	Mediterranean
9CBadalon	Badalona_03	217741	Yes	High	810	138	25.78	4.39	19	54.66	Mediterranean

2.4.2 Explanatory variables

The particle counts of each transect are divided by the area of the trawl opening (0.2meter) and multiplied by the distance in meters trawled. The area (A) of our 20 cm circular net is calculated by the following formulas: $A=\pi\ r2$ $A=\pi\times0.12$ $A=\pi\times0.12$ $A=0.01\pi$.
Volume sampled in m^2 = 0.0314159265. (m^2 × distance sampled in meters) = Volume in m^3.
This was done to range our values according to our one constant factor, the distance trawled, and to better compare the two samples that exceeded 1000 meters. The relative result does not account for ocean currents, river flow, and weather-related water movements. They do not estimate real m^3 since we did not use a Flow-o-meter for the sampling, but simply puts the data into a framework for interpretation. By dividing each sample particle result by the area in m^3 trawled, we get the number of items per m^3.

2.4.3 Linear models

RStudio was used to explore the data between our explanatory variable, particles per m3, from MP VAT and MP-ACT and a set of variables from our investigations using linear models. The parameters used were inhabitants, industry, visitors, and duration of sampling. The results of the linear models are used to find any indication of our parameters predicting the microplastic content.

3 Results

3.1 The Plastsaq trawl design

The Plastsaq trawl design proposed in this study is very functional for trawling a 0.333 um net from a kayak. It was tested by four volunteer kayakers, Frode Bergan, Gregory Gobiet, Julie Buene & Rolf Thorkaas. As a professional kayaker myself, I can confidently say it fits kayak paddling, operates with safety, and is an added overall value to a kayak tour. It is safe to operate in moderate to bad weather and even promotes safety to other paddlers, as the trawl also acts as a raft and thereby a towing device in case of emergencies. Having a quick-release system on the person towing the Plastsaq is essential for safety. If the kayaker releases the Plastsaq in case of emergency, the Plastsaq floats naturally. It has a simple design and could be replicated using sustainable materials. It acquires samples in a wide array of nearshore environments and sanctuaries. It can sample wherever a kayaker can go, even in marine matrixes close to icebergs and ice edges, and for wildlife sanctuary surveys. The design we opted for has the same circular opening as a conventional plankton trawl, 20 cm, which is an advantage because we can transfer the knowledge from plankton trawling and apply it to Plastsaq samples.

3.2 Comparison of MP VAT vs. MP-ACT scripts in ImageJ

The two scripts, MP VAT and MP-ACT were compared (figure 26). The scripts are the result of research by Prata et al. (2019, 2020). We have applied their scripts to our Nile red-stained images. The result of the two scripts is visually compared in figure 12 using the data of table 3. MP-ACT shows the highest overall particle count with 23840 total particles and MP-VAT with 18563 total particles. Despite MP-ACT´s higher overall output, MP-VAT is noted to overestimate or underestimate particle count if the exposure level varies from the imagery in the Nile red-stained images. For example, in the transect with most particles, Gvarv 01, MP-ACT identifies 2482 particles, and MP-VAT identifies 2823 particles. The highest observed difference between the data models is in the Seljord 02 samples. Here MP-ACT identifies 364 particles, and MP-VAT identifies 1245 particles. The least amount of microplastic was detected in Notodden 03, where MP-ACT identifies 103 particles and MP-VAT identifies 120. There are filters where MP-ACT identifies more particles than MP-VAT – for instance, the Gibraltar 03 filters where MP-ACT identifies 1077 particles and MP-VAT identifies 222 particles.

MP-ACT identifies an estimated average of 26,48 particles per m^3. MP-VAT identifies an estimated average of 20,03 particles per m^3. Only through MP-ACT do we get meaningful measurements of

area size, where MP-ACT identifies a total area of 704,86 mm^2 of plastic particles, with an average of 25,17 mm^2 of microplastic across our samples. For further data investigation, we are showing the results of both data models as both have their advantages and disadvantages. Our data investigation suggests that MP-ACT, with visual modification of threshold levels according to exposure and drawing to connect particles, was more suited to our study and more consistent at quantification under our slightly varying image exposures. MP-ACT has the added value of area estimation and the possibility of drawing together particles and, by doing so, better constraining the number of particles. In comparison, MP-VAT is standardized and has the advantage of replicability and objectivity across different observers or laboratories.

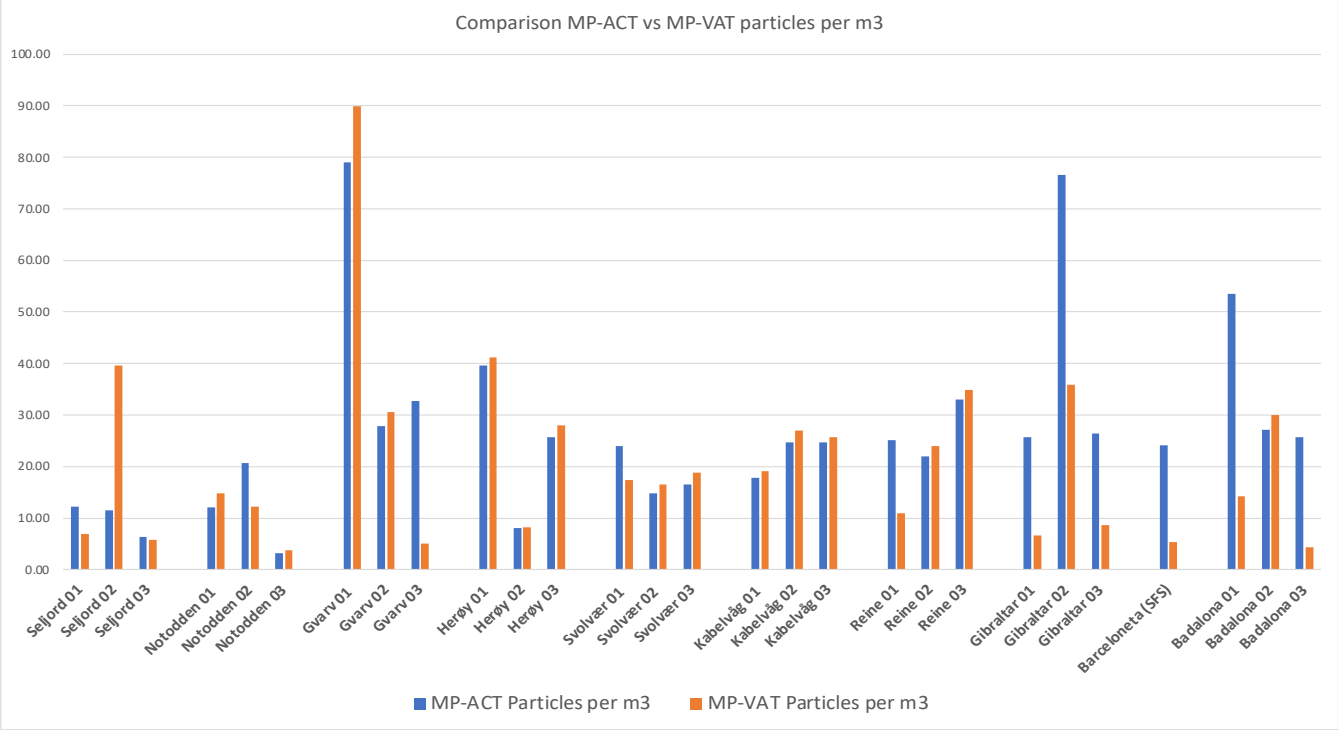

Figure 27 - Histogram comparison of the two data results from MP-ACT and MP-VAT. Histogram created in excel.

3.3 Microplastic differences across sample locations

MP-ACT identifies the Mediterranean as having the highest microplastic concentration average when the samples are grouped together with 37.03 particles per m^3, followed by the southern Norway samples with 23.26 particles per m^3 and then arctic Norway with 22.55 particles per m^3. While MP-VAT identifies southern Norway as having the highest microplastic concentration average with 23.84 particles per m^3, then artic Norway with 21.64 particles per m^3 and the Mediterranean with 15.04 particles per m^3.

The data is treated in RStudio to better understand through visualized in figure 28 and 29. To compare the different sample areas of microplastics, we joined the quantified areas of the microplastic into groups of 3 replicas to represent one location e.g., Seljord. And performed plots to visualize how the data distributes in relation to the other locations. Then the data was grouped to show the difference in latitudes in figure 28 and 29, Southern Norway, Arctic Norway, and the Mediterranean.

Table 3 - the dataset presented as results and used for visualizations and RStudio analysis.

Sampling	Location	MPACT_Particles_pr_m3	MPVAT_Particles_pr_m3	Duration_min	Inhabitants	Industry	Visitors	Total_Particles_MPACT	Total_Particles_MPVAT	Total_MP_Area_mm	Latitude
Seljord_01	1Seljord	12.22	6.88	17	1430	No	Little	384	216	7.46	South.Norway
Seljord_02	1Seljord	11.59	39.63	19	1430	No	Little	364	1245	9.99	South.Norway
Seljord_03	1Seljord	6.33	5.79	19	1430	No	Little	199	182	2.22	South.Norway
Notodden_01	2Notodden	12.13	14.77	18	9024	Yes	Little	381	464	16.11	South.Norway
Notodden_02	2Notodden	20.69	12.22	17	9024	Yes	Little	650	384	25.71	South.Norway
Notodden_03	2Notodden	3.28	3.82	16	9024	Yes	Little	103	120	4.26	South.Norway
Gvarv_01	3Gvarv	79	89.86	21	1082	No	Little	2482	2823	57.54	South.Norway
Gvarv_02	3Gvarv	27.92	30.65	21	1082	No	Little	877	963	16.53	South.Norway
Gvarv_03	3Gvarv	32.69	5.06	20	1082	No	Little	1027	159	24.71	South.Norway
Heroy_01	4Heroy	39.57	41.16	19	49265	Yes	Little	1243	1293	16.99	South.Norway
Heroy_02	4Heroy	8.05	8.24	16	49265	Yes	Little	253	259	3.3	South.Norway
Heroy_03	4Heroy	25.69	28.01	17	49265	Yes	Little	807	880	19.28	South.Norway
Svolvar_01	5Svolvar	24	17.48	16	4714	Yes	Medium	754	549	22.92	Arctic.Norway
Svolvar_02	5Svolvar	14.87	16.62	16	4714	Yes	Medium	467	522	14.92	Arctic.Norway
Svolvar_03	5Svolvar	16.58	18.84	8	4714	Yes	Medium	521	592	20.39	Arctic.Norway
Kabelvag_01	6Kabelvag	17.86	19.16	20	2203	No	Medium	561	602	9.92	Arctic.Norway
Kabelvag_02	6Kabelvag	24.73	27.02	20	2203	No	Medium	777	849	16.86	Arctic.Norway
Kabelvag_03	6Kabelvag	24.76	25.69	20	2203	No	Medium	778	807	8.16	Arctic.Norway
Reine_01	7Reine	25.11	11.01	20	311	Yes	Medium	789	346	8.52	Arctic.Norway
Reine_02	7Reine	22	24.06	20	311	Yes	Medium	691	756	8.12	Arctic.Norway
Reine_03	7Reine	33.04	34.85	20	311	Yes	Medium	1038	1095	9.7	Arctic.Norway
Gibraltar_01	8Gibraltar	25.78	6.65	19	206701	Yes	High	810	209	10.63	Mediterranean
Gibraltar_02	8Gibraltar	76.59	35.87	20	206701	Yes	High	2406	1127	38.75	Mediterranean
Gibraltar_03	8Gibraltar	26.37	8.69	17	206701	Yes	High	1077	355	25.46	Mediterranean
Barceloneta	9Barceloneta	24.08	5.37	110	1620000	Yes	High	1059	236	168.44	Mediterranean
Badalona_01	Badalona	53.48	14.29	19	217741	Yes	High	1680	449	57.22	Mediterranean
Badalona_02	Badalona	27.12	30.02	23	217741	Yes	High	852	943	26.09	Mediterranean
Badalona_03	Badalona	25.78	4.39	19	217741	Yes	High	810	138	54.66	Mediterranean

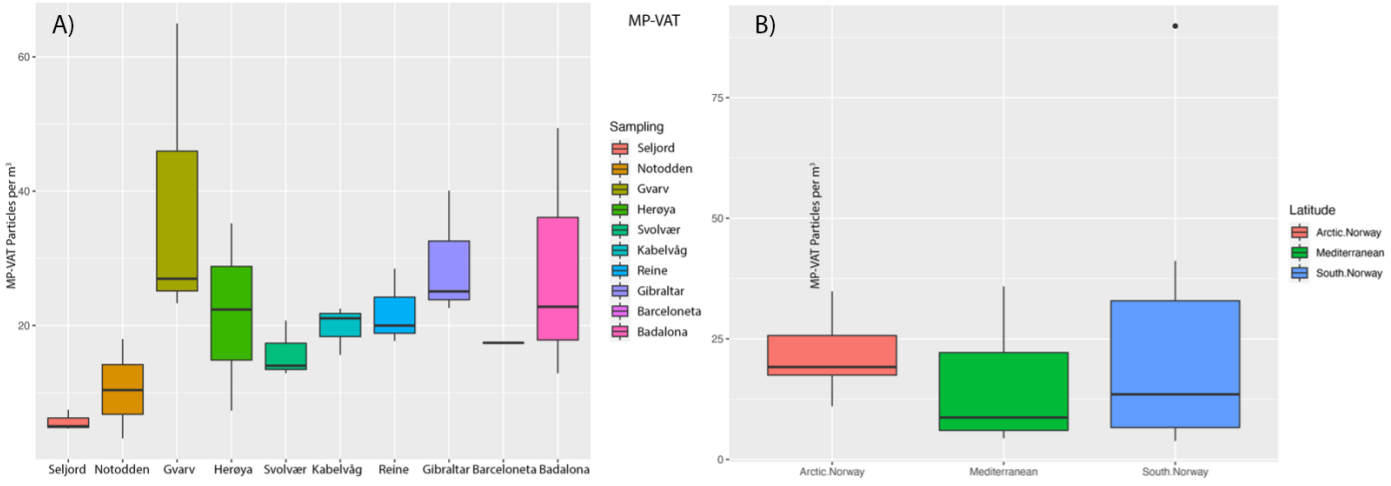

Figure 28 – Boxplot interpretation of data results from MP-VAT. A) Boxplot of results from MP-VAT when the three samples from one area are grouped together into 3 replicas of one location. B) MP-VAT particles per m^3 boxplots of samples grouped into latitude regions. South Norway refers to the freshwater lakes of Telemark. Arctic Norway refers to the marine samples from

Lofoten, Northern Norway and the Mediterranean refers to the samples taken in Gibraltar, Badalona and Barceloneta. Boxplots are created in RStudio.

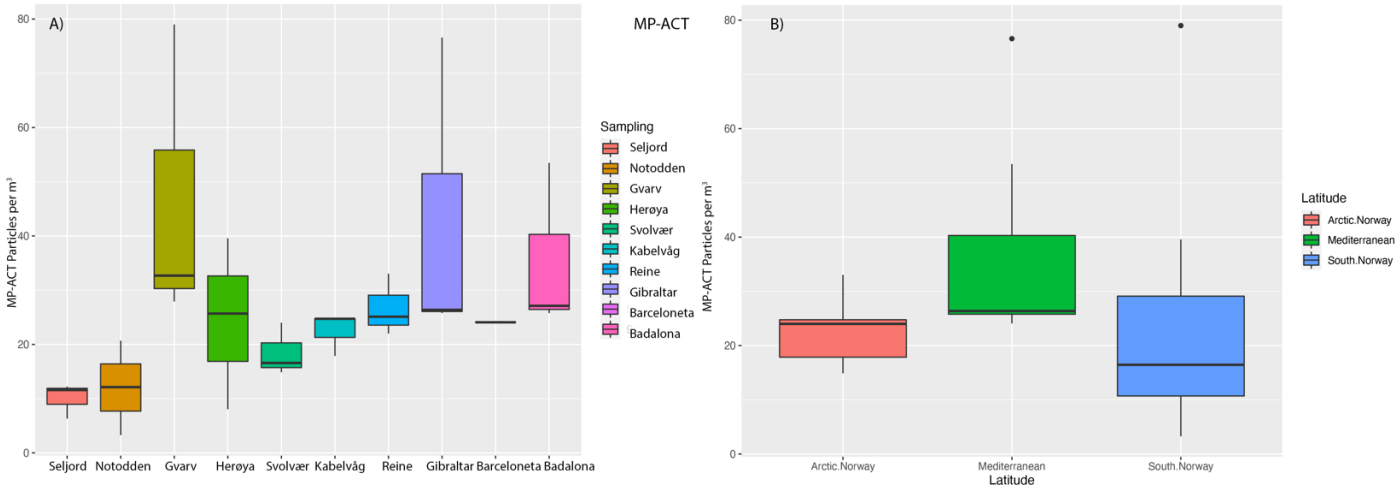

Figure 29 – Boxplot interpretation of data results from MP-ACT. A) Boxplot of results from MP-ACT when the three samples from one area are grouped together into 3 replicas of one location. B) MP-ACT particles per m^3 boxplots of samples grouped into latitude regions. South Norway refers to the freshwater lakes of Telemark. Arctic Norway refers to the marine samples from Lofoten, Northern Norway and the Mediterranean refers to the samples taken in Gibraltar, Badalona and Barceloneta. Boxplots are created in RStudio.

Then to understand the measured area of microplastic, the MP-ACT area is visualized in a histogram in figure 30.

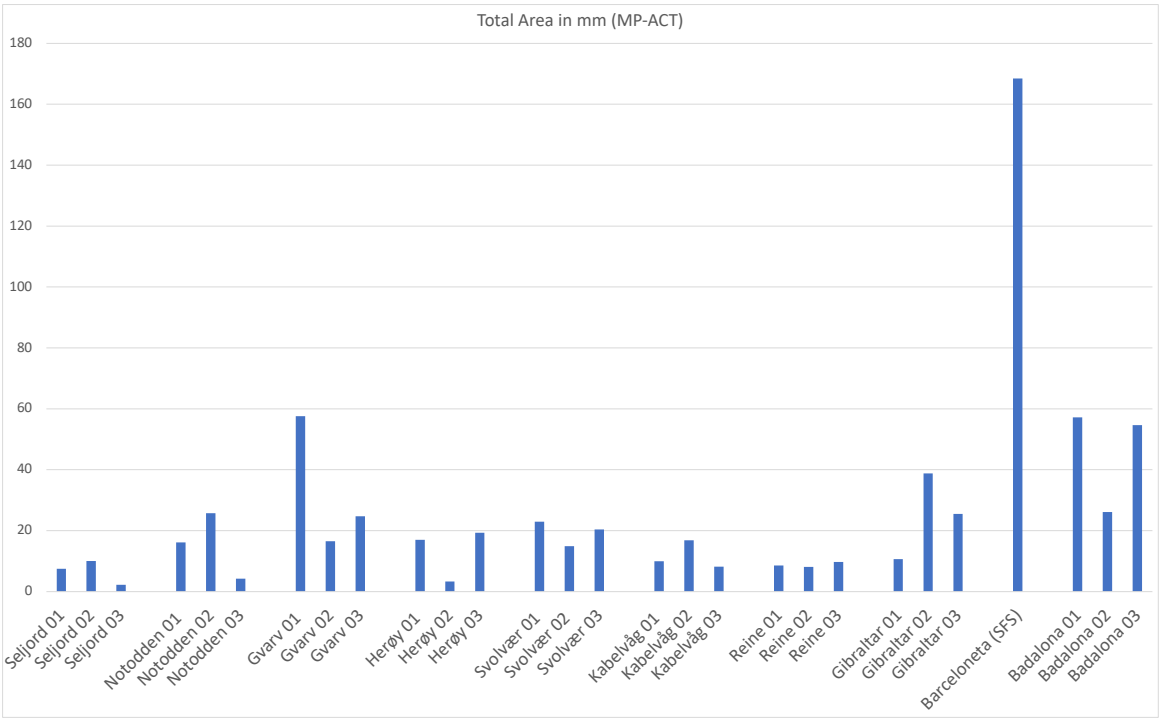

Figure 30 The total area measured for all particles combined from each sample. Histogram created in excel.

3.4 Linear models

All predictor variables failed to explain the concentration of microplastic from the samples. Although p values were insignificant, there are indications of possible relations between inhabitants, industry, and visitor level. The results from linear models are testament to the curiosity that large scale samples might produce. The results from R (RCoreTeam, 2017) from the linear models from the two scripts MP-ACT and MP-VAT are found in supplementary materials.

3.5 FT-IR verification

We have analyzed the spectrum images through 2 open-source programs, openspecy.org and the "know-it-all student" edition. The first 25 particles were determined as plastic polymers by the professional staff. Liam taught me how to run the data through the open-source programs based on books such as the Workman Jr (2000) was given to me by Liam de Haan (UIB) who helped me analyze the Spectro images and determine if the sample was a type of plastic polymer, we only choose to verify yes of no to plastic polymer. The science of spectrometry is fascinating to learn about, the ability to classify and determinate plastic polymers through spectroscopy is something that Nile red analysis can benefit greatly from, I have compiled the evidence into Table 4. The two samples that were not identified as plastic polymers was from the adherent study (Thorkaas, 2022) and river samples from there.

Table 4 - The comprised results of the FTIR particles from Plastsaq samples. Compound estimate is referring to best estimate in collaboration with William De Haan and the FT-IR operators. All particles from our samples of large particles were plastic polymers. In addition to the professional interpretation of particles we used two open-source programs to identify most likely 2nd and estimate of particle type.

Sample	Determined as Plastic Polymer	Polymer1	Score1	Sample_	Author1	Polymer2	Score2	Sample_num
A1	Yes	PET	0.83	623	Suja Sukuma	sealing ring Gardena 1124 large	0.81	326
A1,2	Yes	PET	0.87	623	Suja Sukuma	fibre linen	0.85	389
A2	Yes	PE with silicate inorganic	0.87	617	Suja Sukuma	PE+silicate+bio	0.86	616
A4	Yes	HDPE	0.89	10	Chabuka et a	polyethylene	0.88	609
A5	Yes	polyurethane acrylic resin	0.94	380	Primpke et al.	polyurethane	0.93	501
A6	Yes	polypropylene	0.95	589	Primpke et al.	fibre polypropylene	0.95	494
A9	Yes	polyethylene high density	0.99	355	Primpke et al.	polyethylene high density	0.99	541
A 10	Yes	PET	0.76	238	Chabuka et a	PET	0.75	240
A 12	Yes	polyethylene low density	0.99	584	Primpke et al.	polyethylene high density	0.98	541
B1	Yes	poly(vinyl stearate)	0.86	470	Primpke et al.	ethylene ethyl acrylate	0.82	340
B2	Yes	Polyethylene	0.38	602	Suja Sukuma	HDPE	0.36	48
B2-2	Yes	polyethylene high density	0.99	542	Primpke et al.	polyethylene high density	0.99	541
b3	Yes	polyamide 66	0.78	585	Primpke et al.	polyamide	0.77	545
B5	Yes	alkyd varnish	0.86	361	Primpke et al.	alkyd varnish	0.84	395
B6	Yes	PET	0.78	623	Suja Sukuma	PE with silicate inorganic	0.72	617
B7	Yes	PET	0.78	623	Suja Sukuma	PE with silicate inorganic	0.72	617
B8	Yes	alkyd varnish	0.89	361	Primpke et al.	alkyd varnish	0.87	360
B10	Yes	polyamide 66	0.78	585	Primpke et al.	copolyamide	0.72	543
B11	Yes	broodcomb once brooded	0.78	366	Primpke et al.	HDPE	0.78	127
B12	Yes	polyethylene high density	0.98	541	Primpke et al.	polyethylene high density	0.98	355
C1	Yes	polyamide 66	0.78	585	Primpke et al.	copolyamide	0.78	543
C2	Yes	HDPE	0.81	127	Chabuka et a	PE+silicate+bio	0.78	616
C3	Yes	HDPE	0.66	94	Chabuka et a	fibre viscose	0.65	572
C4	Yes	polyethylene	0.73	609	Suja Sukuma	Polyethylene	0.73	629
C5	Yes	Polypropylene with silicate mix	0.94	630	Suja Sukuma	papercup_cellulosic	0.52	608
C5-2	Yes	Polypropylene with silicate mix	0.94	630	Suja Sukuma	fibre viscose	0.94	572
C6	Yes	polyethylene low density	0.99	584	Primpke et al.	polyethylene high density	0.99	541
C7	**No**	Cardboard/cellulose	0.86	601	Suja Sukuma	cellulose	0.85	624
C8	Yes	PE+silicate+bio	0.74	616	Suja Sukuma	PE with silicate inorganic	0.74	617
C9	Yes	Polypropylene with silicate mix	0.89	601	Suja Sukuma	resin dispersion	0.86	624
C10	**No**	leaf-plant-	0.87	623	Suja Sukuma	fibre linen	0.85	389
C11	Yes	fiberglass	0.97	354	Primpke et al.	fibre flax	0.96	351
D1	Yes	Polypropylene with silicate mix	0.89	601	Suja Sukuma	cellulose	0.86	624
D2	Yes	PE+silicate+bio	0.9	616	Suja Sukuma	PE with silicate inorganic	0.9	617
D3	Yes	PE+silicate+bio	0.83	616	Suja Sukuma	PE with silicate inorganic	0.83	617
BACKGROUND	No							
BACKGROUNDB12	No							
BACKGROUNDC3	No							
BGC7	No							
BGD1	No							
BGFINAL	No							

3.5.1 Contamination filters:

The results from the open-air contamination filters were 76 particles when ran through MP-ACT and 84 through MP-VAT. Both material types of kayaks, PE, and glass fiber, are bright fluorescent under crimelight wavelengths, and could be a source of contamination. Hemp rope, and cardboard box are not fluorescent. Thorkaas (2022) investigated filters where we just ran the KOH: NaClO solution through and found 312 particles using the MP-ACT script in ImageJ.

4 Discussion

The resulting Nile red stained samples of this study are compelling evidence of humankind's discarded surplus in natural environments, plastic debris. Research wants to increase data coverage on environmental microplastics. To achieve that we need rapid, reliable, replicable, and objective ways to obtain data in a wide array of environmental matrixes, both in marine and freshwater. This proof-of-concept microplastics study is performed on already established methods of quantification, by implementing them, evaluating them, and using the obtained knowledge to peer into the future of how this project might evolve over the next decades. The quantification method will surely develop over the next years, but we now have a way of gathering surface water samples via images that can be restudied, from a wide array of previously unstudied locations. The tangible result of this study is the implementation and experimentation with Nile red fluorescent tagging at our university and the microplastic sampling trawl, the Plastsaq. The Nile red-stained images have been quantified to microplastic particles per m^3 via MP-ACT and MP-VAT. This study is only the first stage of a plan to expand microplastic research significantly. The roadmap ahead is implementing all the proposed optimizations after the release of this study and aim for a citizen science implementation by 2023. By implementing considerations and optimizations we hope to increase the value of the data and identifying improvements in the sample design and equipment prior to sampling in eastern Greenland in the summer of 2022.

Our two models, MP-ACT and MP-VAT, show similar and comparable results that quantify the concentration of plastic pollution in the sampled areas. Working with the scripts, they are observed to select only bright fluorescent parts of the images and count particles, thereby quantify microplastics to a satisfactory degree. Aside from minor fragmentation of the edges of larger particles, the actual count of particles is evidently close to the fluorescent particles present in the samples. The following considerations are recommended to heighten the precision and comparability of the two scripts, MP-ACT and MP-VAT. Photographic equipment should be set to all manual so that operators can control both shutter time, ISO (sensitivity to light) and the lens aperture. The equipment should be placed in a Blackbox that shields the sample from other light sources than the Crimelight. The variance of exposure in our images is caused by not being able to control ISO on the school's microscope, it was set to auto low ISO, and could not be changed. ISO auto low results in fluctuating ISO levels when very bright particles are present in samples. Both Maes (2017), Prata et al. (2020) use regular digital cameras, which have the advantage of being easy to manually adjust, small and more cost-effective. A smaller camera setup with modern high-resolution cameras and a ring-light crimelight emitter

attached to the lens is thus recommended. The placement of the Crimelight is important because our images suggest that Nile red does not illuminate all parts of stained particles equally but appears to be mainly illuminating the angles of plastic particles that match the source of light and lens. The recommended placement of the crimelight emitter would be a ring-light, illuminating the sample directly from around the lens, as Meyers et al. (2022) propose. Another method would be placing the samples inside a box of mirrors, so that the crimelight is reflected and diffused onto the sample. This would likely heighten the precision of area measurements as well.

To investigate the microplastic concentration differences between the two scripts, first, it is observed where MP-ACT and MP-VAT disagree the most in figure 27. In some samples, MP-ACT and MP-VAT are significantly different, but in most samples, they identify similar concentrations of microplastic. That is in the samples of Seljord 02, Gvarv 03, Reine 01, Barceloneta, Badalona 01 and 03. Then the Nile red stained filter images connected with the discrepancies for these samples were inspected (images of all the Nile red stained filter images are found in supplementary material). The process unveils why the software count, in this study, improves by human input for a variety of reasons which helps improve Nile red quantification for future studies.

The first discrepancy between the two scripts is at Seljord 02, where MP-VAT estimates much higher microplastic concentrations than MP-ACT. The sample filter in question is almost clean of fluorescent particles, but the image appears slightly unfocused. MP-VAT´s selection includes background noise from the filter, corrupting its estimate. The likely cause of the discrepancy is slight overexposure of the image and the unfocused image. The following discrepancy is at Gvarv 03 here. MP-VAT estimates much lower concentrations than MP-ACT. From visual inspection, Gvarv 03 appears to have fewer particles than the other two samples at Gvarv. The image is slightly underexposed compared to the other two. Reine 01 appears to have many green particles present in the image, while Reine 03 has many red particles. Based on visual inspection, Reine 01 should have comparable results to Reine 02. The Gibraltar samples appear all underexposed, and it seems to be reflected in the results from MP-VAT. The filters contain many green particles. It is observed that MP-VAT is sensitive to exposure and appears to underestimate concentration when many green, fluorescent particles are present. At Barceloneta, MP-VAT estimates a low quantity of microplastic. MP-VAT did not perform well in identifying the larger removed objects from the trawl due to fluorescence differences in the plastic. The threshold imposed by MP-VAT overlooks many bright parts of the images. The likely cause of the discrepancy is exposure variations. MP-VAT poorly identifies the larger particles obtained in the sample, which could only be done using MP-ACT´s

drawing option. The likely cause of the discrepancy is the placement of Crimelight at a singular angle and a slightly underexposed photo. The next disagreement is at the Badalona samples 01 and 03. Consulting the images, they are all well exposed and contain many fluorescent particles. The likely cause of the discrepancy is the presence of many very bright green particles. The threshold imposed by MP-VAT is set too low because of underexposure. When we have many bright fluorescent objects, as in Badalona 03, MP-VAT underestimates when the photos are slightly underexposed.
The highest sample was Gvarv 01, which is curious. Mainly because of the river at the other end, the Seljord samples had a low concentration. Both models indicate a high value for Gvarv 01, which is also evident from visual inspection of the images. The image has a lot of fluorescent areas. It is worth noticing that the Gvarv samples are sampled during a different time of year compared to the rest of the southern Norway samples, and only the first transect, Gvarv 01, shows high results. This should be further investigated by sampling the same stretch again. Our sampling was designed to sample in parallel lines, starting closest to a suspected source of microplastics. It is therefore interesting to observe in which locations the first sample was the highest. That is, via MP-ACT in Seljord, despite two filters being discard, in Notodden, in Gvarv, in Herøya and Svolvær. And via MP-VAT in Gvarv and Herøya. This indicates that microplastics originate from riverine inputs, and that Svolvær harbor releases microplastic to the surrounding marine sea. More data is needed to confirm this.

This study has investigated a simple way to extract data on microplastic via the proposed trawl, the Plastsaq microplastic sampler. It went through four prototype modifications to develop, but the result is a microplastic sampler that´s truly functional. It is specifically designed for the motion and handling of a kayak paddler. Its functionality is demonstrated through the practical employment on the ten kayak tours the samples are a result of. It performs well with handling tasks such as employment, sampling, and sample collection. To accurately measure particles per m^2 or m^3, we need to attach a mechanical Flow-o-meter to the trawl. (Camins et al., 2020) found that through flow-o-meter measurements, that calculating m^2 or m^3, underestimates by about 10%. But having a flow-o-meter permanently attached to the Plastsaq would not cause problems. When trawling with average paddling speed, the net filters particles into the cod-end as desired. It has shown good performance with trawling speeds microplastic between 2 km/h up to 7 km/h (1-3 knots). The Plastsaq could significantly increase data collection in nearshore surface layers via a citizen science framework. There are many good examples of successful citizen science projects on plastics (Jambeck et al., 2015b; Barrows et al., 2018; Compas et al., 2018; Forrest et al., 2019; Rambonnet et al., 2019; Camins et al., 2020). They all are testament that citizen engagement provides reliable environmental data while engaging the public.

Research has no plan to effectively and extensively sample microplastic in many littoral and populated areas, especially at higher latitudes and the arctic. Microplastic is observed be transported to the arctic at a disproportionate high degree, due to atmospheric transport and the pathways of the great ocean-currents (Huserbråten et al., 2022). The ocean-based transportation of floating plastic to the arctic is accelerated with wind and wave-driven Stokes drift and the major thermohaline currents acting as conveyor belts of floating plastic debris to the arctic (Cózar et al., 2017). Plastic in the arctic act as an additional stressor to global warming as Bergmann et al. (2022) reports, they have found early evidence of a relation between arctic plastic pollution and climate change, as depicted in their new assessment of arctic marine litter. The data coverage on microplastic is increasingly sparse in the arctic (Mallory et al., 2021). This study can help solve the lack of data in the arctic because kayaking began there. Both a kayak and the Plastsaq is made for sampling quietly, without disturbing wildlife in arctic environments. The Plastsaq could quickly be adapted to high latitude microplastic research and solve the need of data coverage while adding a modern purpose to kayaking. The Plastsaq´s future include sampling microplastics in Tasiilaq, eastern Greenlandic in the summer of 2022, to further prove the Plastsaq´s usability in arctic environments and help further the findings of Bergmann et al. (2022). Future surveys with the Plastsaq are planned to sample the release of air-transported microplastic in front of glacial drift ice or in front of meltwater rivers from glaciers, both concepts are planned in eastern Greenland. Our study design of trawling one kilometer from a kayak could be utilized in many ways and places e.g., to perform temporal studies, with perhaps the same stretch sampled one time per week throughout a year. This could easily be achieved by kayak clubs or kayak tourism operators who could use the Plastsaq as part of their weekly tours. Both scenarios would create temporal data via large-scale citizen science collaborations. By providing and teaching communities of kayakers how to sample microplastic, we could map many places in Norway and worldwide. Kayak communities could use the Plastsaq as a part of planned kayak activities. Large-scale citizen science project with the Plastsaq would be relatively easy to create with funding and a team behind it. Many communities and locations would benefit from monitoring and several communities have expressed interest in doing so.

Nile red-tagging technique has become an increasingly popular method to identify environmental microplastics in a wide array of matrixes, from sediment, biota, and in the water column (Shim et al., 2016; Shruti et al., 2022). The review done by Shruti et al. (2022) about research in Nile red and microplastics conveys the difference in methods to ascertain data from the stained samples. We have followed the methods suggested by Prata et al. (2020) but many different methods can be applied. A

new study by (Meyers et al., 2022) shows a promising methodology to identify plastic polymers through color recognition in Nile red-stained filters through machine learning based, semi-automated scripts. This slightly altered way of photographing the filters through three different colored filters appears promising. Meyers et al. (2022) use Nile red to not only quantify but also identify plastic polymers. This shows a promising direction that Nile red research is progressing towards, the ability to get more data from the fluorescent tagging. Moreover, their data is also delivered in a simple rapid-screening way, as suggested by Maes (2017). In all areas of microplastic research, there is a need for harmonized, standardized ways of monitoring microplastic. The images and results of this study are available for future reference.

The hardest part of this master's study was selecting a good technique to quantify the Nile red-stained image. The MP-VAT method (J. Prata et al., 2019) does not include detection of the polymers in our samples, excluding some information from Nile red-stained images. We observed that through Nile red staining, polar polymers like nylon and PET fluoresce red, while hydrophobic polymers like PE, PP, and PS fluoresce yellow. This is consistent with the finding of Maes (2017), but there might be even more distinctions to be made within the hydrophobic color range. But exploring that further was out of range of this study. Future Nile red efforts should create comparable laboratory conditions and a harmonized rapid-screening methodology. We are presenting microscopic particles down to 1 µm surface area, far below our mesh net size of 0,333 µm. Arguably, the presented results should have discarded all particles under the mesh size range. We have included all identified particles because the plastic debris initially caught appears to have fragmented during our laboratory treatments with biological matter removal with KOH: NaClO solution, this is observed by the incredible amount of small fluorescent particles in the Images. To demonstrate that with the Nile Red fluorescent technique, you can quantify plastic microplastic at the nano plastic range. The lowest identifiable particle one can detect is related to photographic magnification and Nile red chemical composition. But it is also observed that increasing the threshold of an image increases the smallest particles in the image. This could be accounted for and tested by running imagery analysis with high and low thresholds and taking away particles under a specific size, based on the results of low threshold.

Several size range limitations were tested in the background of this data presented by removing particles with areas <0.001 and <0.001 mm^2 from the data, also with limitations within the feret sizes measured, feret size might be the best indicator of area of particles in relation to the mesh size of the Plastsaq. Doing so can reveal new patterns of only the big particles present in our samples. Using our collected data, one can make to make more statistics on the information given by the scripts. It

provides data on distribution of either particle, fiber or fragment. But since particles appear fragmented in our data, the estimation did not appear meaningful to present and all are presented as particles.

This study is the first proof-of-concept study at our university using Nile red. We did not have a microplastic cleanroom or designated lab. We had ordinary lab facilities. So, a degree of contamination is to be expected. However, we have used the utmost care to cleanse our sample equipment with acetone and use distilled water to pre-and post-rinse all laboratory equipment. We had a contamination filter open whenever we treated the samples and had the filter exposed to the open air of the lab. Over many weeks, this filter contained 76 particles. Which spread over the 44 filters is 1.7 particles per filter, making the case that dedicated laboratories should be created where the post-sampling contamination is minimized. Both kayaks could be prone to contamination as their PE body and glass fiber coating are strongly fluorescent. Kayaking itself could be a potential source of plastic. This should be further tested, but the contamination concern is minimal as a floating kayak should not shed mass unless hitting rocks or objects in the water. When sampling, an 8-meter distance between the Plastsaq and the kayaker limits this contamination concern. Another concern is the addition of plastic particles from the laboratory equipment used. In the adherent bachelor thesis study, hundreds of fluorescent particles were detected in the KOH: NaClO solution container. All liquids, including KOH: NaCLO and distilled water, should have been pre-filtered in this study.

The density separation technique using ZnCl, as proposed by Maes (2017), was used for only three samples in this study. However, the data shows comparable results to others, and the density separation technique is recommended for future utilization of the Nile red, especially when having samples with low content of biological matter. In our study, all samples from the marine arctic have had low biological matter content, and density separation could have been used. However, the freshwater samples of southern Norway and the Mediterranean samples were so high in biological matter that biological digestion was needed. It is worth noticing that ZnCl is biologically more sustainable than KOH: NaClO and more cost-efficient. The density of the ZnCl concentration might need to be based on the floating plastic being collected from marine or freshwater samples.

There are significant differences in how researchers sample, extract and quantify microplastics across the world (Hidalgo-Ruz et al., 2012b). Our understanding of accumulation patterns and pathways for floating marine plastic is expanding as science unveils new patterns, recent papers discuss the quantities of environmental plastic largely secluded to beaches, big open seas, and coastal areas

(Cozar et al., 2014; Van Sebille et al., 2020). Far less is known of the nearshore areas, both freshwater and marine, of the breakwater zones areas and river outflows. As research tries to map and understand plastics effects on the ecosystems, it is clear that research needs larger datasets to work with, as exampled in the recent review by Bucci et al. (2020). The study calls for global studies on microplastic, with study designs that test how microplastic exists as polymers, their shapes, sizes, and concentrations and how that may affect wildlife. My argument is that if we want to understand microplastics' effect on wildlife, we need to increase our data sets significantly. To find background references of concentration and collaborate through temporal studies with large data sets with solid parameters and observations. To perhaps see which effects may show when concentrations are the highest or other environmental parameters are included. Plastics in natural habitats are observed to be ubiquitously distributed and considered a permanent pollutant of emerging global concern that needs more data to fully document the ecological, economic, and environmental impacts plastic has (Barnes et al., 2009; Thompson et al., 2009), some argue, that we already have passed the threshold of plastic concentrations to ensure a thriving ecosystem within our planetary boundaries (Persson et al., 2022).

Regarding further studies and Nile red validation at USN, the limit of detection and limit of quantitation at USN should be defined by using standard deviation measured from many blank filters stained with Nile red using filtered liquids and adding contamination data across all sections of the laboratory process with Nile red at USN. The limit of limit of detection, would be three times the standard deviation of blank filters + the measured contamination. The limit of quantitation would be ten times the standard deviation of blank filters + the measured contamination, this could be subtracted from the results of this study. We emphasize the need to develop global standard protocols to treat and retrieve data on microplastic samples. We now have the state-of-the-art equipment to perform Nile red analysis at our facilities and paving a way to lower the costs of Norwegian microplastic extent and research. The result of this thesis paves the way for widespread and informative microplastic research. The technique developed and implemented at USN Bø could be a valuable agent for increasing data coverage on aquatic environmental microplastics. The data reveals very high output from Gvarv 01, why is that? Future studies may benefit from open research questions based on the big observed difference in microplastic concentration from Seljordsvannet at one end of the river of Bø (Bøelva) and Norsjø with the settlement Gvarv in the other end of the river and using the quantification using Nile red. Further development of MP-VAT2.0 (Prata et al., 2020) is wanted, to also include an MP-ACT 2.0, that allows threshold adjustment according to exposure and a plan for polymer identification through colors. Future studies might benefit from investigating other

methods of quantifying the Nile red stained samples. The recent study by Meyers et al. (2022) appears promising and could heighten the data value of Nile red stained microplastic samples.

5 Conclusion

This study has explored the field of script-based, rapid-screening approach using Nile red to quantify microplastics. In this proof-of-concept study we have successfully achieved information about nearshore environments in both fresh- and salt-water locations that sprout further research curiosity. To understand the accumulation and behavior patterns of floating plastics, offshore waters have been extensively surveyed while floating microplastics in nearshore surface waters are lacking data coverage and extent. Microplastic data is sparse, especially in the littoral, nearshore areas, owing to the difficulty of conducting microplastic research. Both sample collection and analyzing measures. The inherent small sizes of the study subject, microplastic, its omnipresence and polymer variety make it complicated to quantify. In the open sea, scientific manta-trawls are used for microplastic sampling, and these can only be towed from ships or small boats. To overcome this limitation in sampling coverage, we are presenting a cost-effective way to enhance mapping of nearshore microplastic.

We have designed a kayak trawl to collect samples easily from any location a kayak paddler can get to. The kayak trawl named “Plastsaq” generates samples which can be used with Nile red tagging to pinpoint zones of interests for traditional scientific research on microplastics. The kayak trawl is lightweight, easy to deploy and sample with. The Plastsaq offers a new way to sample arctic, marine, and freshwater microplastics. It increases opportunities to document the abundance and impact of microplastics over time. It could be used in a citizen science network, in a more comprehensive scientific program where citizens are engaged to map microplastics in their nearshore environments. This project has a high potential to leverage the public's interest and awareness about plastic pollution while at the same time generate new monitoring data. Our results reveal that concentration of floating plastics in the nearshore of freshwaters of Southern Norway and those of the marine arctic of Lofoten, Northern Norway, the Gibraltar strait and Barcelona are significant and urges mitigation. We present a way to connect modern day kayaking with a purpose by quantifying surface layer microplastics and we are awaiting constructive critic to improve upon this concept for many years to come.

References

Aliani, S., & Molcard, A. . (2003). Hitch-hiking on floating marine debris: macrobenthic species in the Western Mediterranean Sea. In Migrations and Dispersal of Marine Organisms. *Springer, Dordrecht.*

Andrady, A. L., & Neal, M. A. (2009). Applications and societal benefits of plastics. *Philos Trans R Soc Lond B Biol Sci, 364*(1526).

Barnes, D. K., Galgani, F., Thompson, R. C., & Barlaz, M. (2009). Accumulation and fragmentation of plastic debris in global environments. *Philos Trans R Soc Lond B Biol Sci, 364*(1526).

Barrows, A. P. W., Christiansen, K. S., Bode, E. T., & Hoellein, T. J. (2018). A watershed-scale, citizen science approach to quantifying microplastic concentration in a mixed land-use river. *Water Res, 147*, 382-392.

Bergmann, M., Collard, F., Fabres, J., Gabrielsen, G. W., Provencher, J. F., Rochman, C. M., . . . Tekman, M. B. (2022). Plastic pollution in the Arctic. *Nature Reviews Earth & Environment*, 1-15.

Borrelle, S. B., Ringma, J., Law, K. L., Monnahan, C. C., Lebreton, L., McGivern, A., . . . Rochman, C. M. (2020). Predicted growth in plastic waste exceeds efforts to mitigate plastic pollution. *Science, 369*(6510), 1515-1518.

Botterell, Z. L. R., Beaumont, N., Cole, M., Hopkins, F. E., Steinke, M., Thompson, R. C., & Lindeque, P. K. (2020). Bioavailability of Microplastics to Marine Zooplankton: Effect of Shape and Infochemicals. *Environ Sci Technol, 54*(19), 12024-12033.

Browne, M. A., Galloway, T., & Thompson, R. (2007). Microplastic- an emerging contaminant of potential concern? *Integrated environmental assessment and Management, 3*(4), 559-561.

Bucci, K., Tulio, M., & Rochman, C. (2020). What is known and unknown about the effects of plastic pollution: A meta-analysis and systematic review. *Ecological Applications, 30*(2), e02044.

Camins, E., de Haan, W. P., Salvo, V. S., Canals, M., Raffard, A., & Sanchez-Vidal, A. (2020). Paddle surfing for science on microplastic pollution. *Sci Total Environ, 709*, 136178.

Carpenter, E. J., & Smith, K. L., Jr. (1972). Plastics on the Sargasso sea surface. *Science, 175*(4027), 1240-1.

Cole, M., Lindeque, P., Halsband, C., & Galloway, T. S. (2011). Microplastics as contaminants in the marine environment: a review. *Marine pollution bulletin, 62*(12), 2588-2597.

Compas, E. D., & Wade, S. (2018). Testing the waters: a demonstration of a novel water quality mapping system for citizen science groups. *Citizen Science: Theory and Practice, 3*(2).

Cozar, A., Echevarria, F., Gonzalez-Gordillo, J. I., Irigoien, X., Ubeda, B., Hernandez-Leon, S., . . . Duarte, C. M. (2014). Plastic debris in the open ocean. *Proc Natl Acad Sci U S A, 111*(28), 10239-44.

Cózar, A., Martí, E., Duarte, C. M., García-de-Lomas, J., Van Sebille, E., Ballatore, T. J., . . . Echevarría, F. (2017). The Arctic Ocean as a dead end for floating plastics in the North Atlantic branch of the Thermohaline Circulation. *Science advances, 3*(4).

Eriksen, M., Lebreton, L. C., Carson, H. S., Thiel, M., Moore, C. J., Borerro, J. C., . . . Reisser, J. (2014). Plastic pollution in the world's oceans: more than 5 trillion plastic pieces weighing over 250,000 tons afloat at sea. *PloS one, 9*(12).

Forrest, S. A., Holman, L., Murphy, M., & Vermaire, J. C. (2019). Citizen science sampling programs as a technique for monitoring microplastic pollution: results, lessons learned and recommendations for working with volunteers for monitoring plastic pollution in freshwater ecosystems. *Environmental monitoring and assessment, 191*(3).

GESAMP. (2016). Sources, fate and effects of microplastics in the marine environment, part two of a global assessment. *GESAMP No. 93*.

Geyer, R. (2020). A brief history of plastics. In *Mare Plasticum-The Plastic Sea* (pp. 31-47): Springer.
Greenspan, P., & Fowler, S. D. (1985). Spectrofluorometric studies of the lipid probe, nile red. *J Lipid Res, 26*(7), 781-9.
Harris, P., Tamelander, J., Lyons, Y., Neo, M., & Maes, T. (2021). Taking a mass-balance approach to assess marine plastics in the South China Sea. *Marine pollution bulletin, 171*, 112708.
Hermabessiere, L., Dehaut, A., Paul-Pont, I., Lacroix, C., Jezequel, R., Soudant, P., & Duflos, G. (2017). Occurrence and effects of plastic additives on marine environments and organisms: A review. *Chemosphere, 182*, 781-793.
Hidalgo-Ruz, V., Gutow, L., Thompson, R. C., & Thiel, M. (2012a). Microplastics in the marine environment: a review of the methods used for identification and quantification. *Environ Sci Technol, 46*(6), 3060-75. doi:10.1021/es2031505
Hidalgo-Ruz, V., Gutow, L., Thompson, R. C., & Thiel, M. (2012b). Microplastics in the marine environment: a review of the methods used for identification and quantification. *Environmental science & technology, 46*(6).
Huserbråten, M. B., Hattermann, T., Broms, C., & Albretsen, J. (2022). Trans-polar drift-pathways of riverine European microplastic. *Scientific Reports, 12*(1).
Jambeck, J. R., Geyer, R., Wilcox, C., Siegler, T. R., Perryman, M., Andrady, A., . . . Law, K. L. (2015a). Plastic waste inputs from land into the ocean. *Science, 347*(6223).
Jambeck, J. R., & Johnsen, K. (2015b). Citizen-based litter and marine debris data collection and mapping. *Computing in Science & Engineering, 17*(4).
Jeyasanta, K. I., Sathish, N., Patterson, J., & Edward, J. K. P. (2020). Macro-, meso- and microplastic debris in the beaches of Tuticorin district, Southeast coast of India. *Mar Pollut Bull, 154*, 111055.
Kaiser, D., Kowalski, N., & Waniek, J. J. (2017). Effects of biofouling on the sinking behavior of microplastics. *Environmental Research Letters, 12*(12).
Kanhai, D. K., Gardfeldt, K., Krumpen, T., Thompson, R. C., & O'Connor, I. (2020). Microplastics in sea ice and seawater beneath ice floes from the Arctic Ocean. *Sci Rep, 10*(1).
Kappler, A., Windrich, F., Loder, M. G., Malanin, M., Fischer, D., Labrenz, M., . . . Voit, B. (2015). Identification of microplastics by FTIR and Raman microscopy: a novel silicon filter substrate opens the important spectral range below 1300 cm(-1) for FTIR transmission measurements. *Anal Bioanal Chem, 407*(22).
Kasavan, S., Yusoff, S., Fakri, M. F. R., & Siron, R. (2021). Plastic pollution in water ecosystems: A bibliometric analysis from 2000 to 2020. *Journal of Cleaner Production, 313*, 127946.
Kim, S. K., Lee, H. J., Kim, J. S., Kang, S. H., Yang, E. J., Cho, K. H., . . . Andrady, A. (2021). Importance of seasonal sea ice in the western Arctic ocean to the Arctic and global microplastic budgets. *J Hazard Mater, 418*, 125971.
Koelmans, A. A., Besseling, E., Wegner, A., & Foekema, E. M. (2013). Plastic as a carrier of POPs to aquatic organisms: a model analysis. *Environmental science & technology, 47*(14).
Law, K. L., Moret-Ferguson, S., Maximenko, N. A., Proskurowski, G., Peacock, E. E., Hafner, J., & Reddy, C. M. (2010). Plastic accumulation in the North Atlantic subtropical gyre. *Science, 329*(5996).
Li, W. C., Tse, H. F., & Fok, L. (2016). Plastic waste in the marine environment: A review of sources, occurrence and effects. *Sci Total Environ, 566-567*.
Lv, L., Qu, J., Yu, Z., Chen, D., Zhou, C., Hong, P., . . . Li, C. (2019). A simple method for detecting and quantifying microplastics utilizing fluorescent dyes-Safranine T, fluorescein isophosphate, Nile red based on thermal expansion and contraction property. *Environmental Pollution, 255*.
Maes, T., Jessop, R., Wellner, N., Haupt, K., & Mayes, A. G. . (2017). A rapid-screening approach to detect and quantify microplastics based on fluorescent tagging with Nile Red.pdf. *Nature*.

Mahtani, K., Spencer, E. A., Brassey, J., & Heneghan, C. (2018). Catalogue of bias: observer bias. *BMJ Evid Based Med, 23*(1), 23-24.
Mallory, M. L., Baak, J., Gjerdrum, C., Mallory, O. E., Manley, B., Swan, C., & Provencher, J. F. (2021). Anthropogenic litter in marine waters and coastlines of Arctic Canada and West Greenland. *Science of the Total Environment, 783*.
Meyers, N., Catarino, A. I., Declercq, A. M., Brenan, A., Devriese, L., Vandegehuchte, M., . . . Everaert, G. (2022). Microplastic detection and identification by Nile red staining: Towards a semi-automated, cost- and time-effective technique. *Sci Total Environ, 823*.
Michida, Y., Chavanich, S., Chiba, S., Cordova, M. R., Cozsar Cabanas, A., Glagani, F., . . . Kershaw, P. (2019). Guidelines for Harmonizing Ocean Surface Microplastic Monitoring Methods. Version 1.1.
Napper, I. E., & Thompson, R. C. (2020). Plastic Debris in the Marine Environment: History and Future Challenges. *Glob Chall, 4*(6).
Nerland, I. L., Halsband, C., Allan, I., & Thomas, K. V. (2014). Microplastics in marine environments: occurrence, distribution and effects.
Onink, V., Jongedijk, C. E., Hoffman, M. J., van Sebille, E., & Laufkötter, C. (2021). Global simulations of marine plastic transport show plastic trapping in coastal zones. *Environmental Research Letters, 16*(6).
Persson, L., Carney Almroth, B. M., Collins, C. D., Cornell, S., de Wit, C. A., Diamond, M. L., . . . Hauschild, M. Z. (2022). Outside the Safe Operating Space of the Planetary Boundary for Novel Entities. *Environ Sci Technol, 56*(3).
PlasticsEurope. (2021). *Plastics - the Facts 2021.* Retrieved from https://plasticseurope.org/wp-content/uploads/2021/12/Plastics-the-Facts-2021-web-final.pdf
Prata, J., Alves, J., da Costa, J., Duarte, A., & Rocha-Santos, T. (2020). Major factors influencing the quantification of Nile Red stained microplastics and improved automatic quantification (MP-VAT 2.0). *Sci Total Environ, 719*, 137498. doi:10.1016/j.scitotenv.2020.137498
Rambonnet, L., Vink, S. C., Land-Zandstra, A. M., & Bosker, T. (2019). Making citizen science count: Best practices and challenges of citizen science projects on plastics in aquatic environments. *Mar Pollut Bull, 145*, 271-277.
RCoreTeam. (2017). *R: A language and environment for statistical computing.* Vienna, Austria, R Foundation for Statistical Computing.
Rech, S., Borrell, Y., & García-Vazquez, E. (2016). Marine litter as a vector for non-native species: what we need to know. *Marine pollution bulletin, 113*(1-2).
Reisser, J., Slat, B., Noble, K., Du Plessis, K., Epp, M., Proietti, M., . . . Pattiaratchi, C. (2015). The vertical distribution of buoyant plastics at sea: an observational study in the North Atlantic Gyre. *Biogeosciences, 12*(4).
Sanchez-Vidal, A., Uviedo, O., Higueras, S., Ballesteros, M., Curto, X., de Haan, W. P., . . . Calafat, A. (2021). *Paddle surfing for science on microplastic pollution: a successful citizen science initiative.* Paper presented at the EGU General Assembly Conference Abstracts.
Shim, W. J., Song, Y. K., Hong, S. H., & Jang, M. (2016). Identification and quantification of microplastics using Nile Red staining. *Marine pollution bulletin, 113*(1-2).
Shruti, V., Pérez-Guevara, F., Roy, P. D., & Kutralam-Muniasamy, G. (2022). Analyzing microplastics with Nile Red: Emerging trends, challenges, and prospects. *Journal of Hazardous Materials, 423*, 127171.
Stanton, T., Johnson, M., Nathanail, P., Gomes, R. L., Needham, T., & Burson, A. (2019). Exploring the efficacy of Nile red in microplastic quantification: a costaining approach. *Environmental Science & Technology Letters, 6*(10).
Tagg, A. S., Sapp, M., Harrison, J. P., & Ojeda, J. s. J. (2015). Identification and quantification of microplastics in wastewater using focal plane array-based reflectance micro-FT-IR imaging. *Analytical chemistry, 87*(12).

Thompson, R. C., Moore, C. J., vom Saal, F. S., & Swan, S. H. (2009). Plastics, the environment and human health: current consensus and future trends. *Philos Trans R Soc Lond B Biol Sci, 364*.

Thorkaas, R. (2022). *Nile red metoden for identifikasjon av mikroplast.* The university of south-east Norway, Department Bø.

UNEP. (2022). End plastic pollution: Towards an international legally binding instrument. Retrieved from https://wedocs.unep.org/handle/20.500.11822/38525

Van Sebille, E., Aliani, S., Law, K. L., Maximenko, N., Alsina, J. M., Bagaev, A., . . . Cózar, A. (2020). The physical oceanography of the transport of floating marine debris. *Environmental Research Letters, 15*(2).

Van Sebille, E., England, M. H., & Froyland, G. (2012). Origin, dynamics and evolution of ocean garbage patches from observed surface drifters. *Environmental Research Letters, 7*(4).

Van Sebille, E., Wilcox, C., Lebreton, L., Maximenko, N., Hardesty, B. D., van Franeker, J. A., . . . Law, K. L. (2015). A global inventory of small floating plastic debris. *Environmental Research Letters, 10*(12).

Workman Jr, J. (2000). *The handbook of organic compounds, three-volume set: Nir, ir, r, and uv-vis spectra featuring polymers and surfactants*. Academic Press; 1st edition: Elsevier.

Wright, S. L., Thompson, R. C., & Galloway, T. S. (2013). The physical impacts of microplastics on marine organisms: a review. *Environ Pollut, 178*.

Yin, K., Wang, Y., Zhao, H., Wang, D., Guo, M., Mu, M., . . . Li, J. (2021). A comparative review of microplastics and nanoplastics: toxicity hazards on digestive, reproductive and nervous system. *Science of the Total Environment, 774*.

Ziajahromi, S., Neale, P. A., Rintoul, L., & Leusch, F. D. (2017). Wastewater treatment plants as a pathway for microplastics: development of a new approach to sample wastewater-based microplastics. *Water research, 112*.

Zimmermann, L., Bartosova, Z., Braun, K., Oehlmann, J. r., Völker, C., & Wagner, M. (2021). Plastic products leach chemicals that induce in vitro toxicity under realistic use conditions. *Environmental science & technology, 55*(17).